RESEARCH ARTICLE | *Cellular and Molecular Properties of Neurons*

Differential and synergistic roles of 17β-estradiol and progesterone in modulating adult female rat nucleus accumbens core medium spiny neuron electrophysiology

Stephanie B. Proaño,[1,2,3] Amanda A. Krentzel,[2,3] and John Meitzen[2,3,4]

[1]*Graduate Program in Biology, North Carolina State University, Raleigh, North Carolina;* [2]*W.M. Keck Center for Behavioral Biology, North Carolina State University, Raleigh, North Carolina;* [3]*Department of Biological Sciences, North Carolina State University, Raleigh, North Carolina; and* [4]*Center for Human Health and the Environment, North Carolina State University, Raleigh, North Carolina*

Proaño SB, Krentzel AA, Meitzen J. Differential and synergistic roles of 17β-estradiol and progesterone in modulating adult female rat nucleus accumbens core medium spiny neuron electrophysiology. *J Neurophysiol* 123: 2390–2405, 2020. First published May 13, 2020; doi:10.1152/jn.00157.2020.—Naturally occurring cyclical changes in sex steroid hormones such as 17β-estradiol and progesterone can modulate neuron function and behavior in female mammals. One example is the estrous cycle in rats, which is composed of multiple phases. We previously reported evidence of differences between estrous cycle phases in excitatory synapse and intrinsic electrophysiological properties of rat nucleus accumbens core (AcbC) medium spiny neurons (MSNs). The AcbC is a nexus between the limbic and premotor systems and is integral for controlling motivated and reward-associated behaviors and disorders, which are sensitive to the estrous cycle and hormones. The present study expands our prior findings by testing whether circulating levels of estradiol and progesterone correlate with changes in MSN electrophysiology across estrous cycle phases. As part of this project, the excitatory synapse and intrinsic excitability properties of MSNs in late proestrus of adult female rats were assessed. Circulating levels of estradiol correlate with resting membrane potential, the time constant of the membrane, and rheobase. Circulating levels of progesterone correlate with miniature excitatory postsynaptic current (mEPSC) frequency and amplitude. Circulating levels of estradiol and progesterone together correlate with mEPSC amplitude, resting membrane potential, and input resistance. The late proestrus phase features a prominent and unique decrease in mEPSC frequency. These data indicate that circulating levels of estradiol and progesterone alone or in combination interact with specific MSN electrophysiological properties, indicating differential and synergistic roles of these hormones. Broadly, these findings illustrate the underlying endocrine actions regarding how the estrous cycle modulates MSN electrophysiology.

NEW & NOTEWORTHY This research indicates that estradiol and progesterone act both differentially and synergistically to modulate neuron physiology in the nucleus accumbens core. These actions by specific hormones provide key data indicating the endocrine mechanisms underlying how the estrous cycle modulates neuron physiology in this region. Overall, these data reinforce that hormones are an important influence on neural physiology.

INTRODUCTION

The menstrual cycle in humans and its analogous cycle in rodents, the estrous cycle, influence neuron physiology across multiple brain regions (Adams et al. 2018; Blume et al. 2017; Olmos et al. 1989; Proaño et al. 2018; Terasawa and Timiras 1968; Willett et al. 2019; Woolley and McEwen 1993). Both cycles feature cyclical changes in the circulating levels of ovarian hormones such as 17β-estradiol (estradiol) and progesterone and are divided into distinct phases. These phases are characterized by differing concentrations of estradiol and progesterone as well as by accompanying changes in reproductive organ physiology and associated reproductive behaviors (Beach 1976; Blaustein 2008; Erskine 1989; Hubscher et al. 2005; Kow and Pfaff 1973; Micevych et al. 2017; Westwood 2008). The rat estrous cycle typically occurs over a 4- to 5-day time period and is divided into distinct phases, including diestrus, proestrus, and estrus. Diestrus features relatively low levels of estradiol and progesterone that then gradually begin to rise. Proestrus is when these hormones reach peak circulating levels in a temporally distinct fashion. The morning of proestrus features a surge in circulating levels of estradiol, followed in the afternoon by a surge in circulating levels of progesterone. This differential hormone action, coupled with other physiological processes, allows the proestrus phase to be further subdivided into early and late proestrus phases (also designated proestrus AM and proestrus PM phases) (Adams et al. 2018). The third phase is estrus, when the effects of estradiol and progesterone linger, even though the circulating concentrations are low. Recently, we showed that the excitatory synaptic input and intrinsic excitability properties of nucleus accumbens core (AcbC) medium spiny neurons (MSNs) robustly change across the estrous cycle (diestrus, early proestrus, and estrus) (Proaño et al. 2018). These findings provided the first line of evidence in support of the documented

Correspondence: J. Meitzen (jemeitze@ncsu.edu).

changes in AcbC-mediated behaviors that differentially manifest across the estrous cycle in rodents and the menstrual cycle in humans. These behaviors include those related to motivation, reward and reinforcement, and pathologies such as anxiety, depression, and addiction, which are all regulated by the AcbC (Becker and Hu 2008; Becker et al. 2001; Evans and Foltin 2006; Lebron-Milad and Milad 2012; Milad et al. 2009).

The AcbC is a highly conserved brain region that serves as a nexus between the limbic and premotor systems that manages the cognitive processing of motivation, reward, and reinforcement (Floresco 2015; Francis and Lobo 2017). It receives glutamatergic inputs from prefrontal cortex, amygdala, and hippocampus and dopaminergic inputs from the ventral tegmental area (Deroche et al. 2020; Salgado and Kaplitt 2015), among others. These inputs converge and are then integrated by GABAergic MSNs, the primary output neuron subtype in the AcbC, and, by extension, are part of the reward circuitry of the brain (Salgado and Kaplitt 2015). Recent findings have shown that AcbC MSNs in adulthood express membrane-associated estrogen receptors α, β, and GPER-1 (Almey et al. 2012, 2015, 2016). AcbC dopaminergic and glutamatergic action, such as synapse number, receptor number, and neurotransmitter availability, exhibit sensitivity to estradiol (Becker 1999; Becker et al. 2012; Calipari et al. 2017; Forlano and Woolley 2010; Meisel and Mullins 2006; Mermelstein et al. 1996; Wissman et al. 2012). Furthermore, the AcbC is sensitive to developmental and acute estradiol action (Cao et al. 2016, 2018; Krentzel et al. 2019, 2020; Perry et al. 2013; Tonn Eisinger et al. 2018). In addition to the effects of estradiol, progesterone and its derivatives have been documented to modulate $GABA_A$ receptors by acting as chloride channels, albeit not yet in the AcbC (Backström et al. 2011, 2014). There is select evidence for progesterone receptor expression in the AcbC (Dluzen and Ramirez 1989b; Ke and Ramirez 1990; Piechota et al. 2017; Sterling et al. 1987).

The individual contributions of circulating levels of estradiol and progesterone in the modulation of excitatory synaptic input and intrinsic excitability properties across the estrous cycle in the AcbC is unknown. This is a critical knowledge gap given that the estrous cycle is a natural variable that not only induces robust neural and behavioral changes but is an integral part of adult female physiology of reproductive age. Here we address this question by testing the hypothesis that circulating levels of 17-β estradiol and progesterone, alone or in combination, correlate with changes in MSN electrophysiological properties across the estrous cycle. To accomplish this, we first augmented our existing data set of female rat MSNs in diestrus, early proestrus and estrus (Proaño et al. 2018) by conducting additional whole cell patch-clamp recordings of AcbC MSNs from late proestrus, which has never before been performed by any laboratory group. We then employed a hormone extraction technique to measure 17-β estradiol and progesterone levels from blood serum samples obtained at euthanasia from rats in all phases of the estrous cycle. Using this expanded data set, we then tested whether circulating levels of 17-β estradiol and progesterone correlated with MSN electrophysiological properties.

METHODS

Animals

All animal protocols were approved by the Institutional Animal Care and Use Committees at North Carolina State University. Postnatal day 60 (P60) female Sprague-Dawley CD IGS rats were purchased from Charles River Laboratories. Rats were housed in pairs until postnatal day 65. After postnatal day 65, animals were individually housed to facilitate assessment of late proestrus ($n = 12$). Animals in other phases were generated in a recent and directly preceding study that employed the same methods as employed in the current study (Proaño et al. 2018). New to this study are animals in late proestrus. For the purposes of this study, late proestrus is defined as the time near the end of the ~12-h proestrus phase, when vaginal cytology exhibits predominantly round and nucleated cells, with initial but minimal appearance of clumped cornified epithelial cells that is characteristic of the estrus phase. In nocturnal animals such as rats, late proestrus typically occurs in the late afternoon of the proestrus phase (Becker et al. 2002). For the purpose of this study, early proestrus is defined as near the beginning of the ~12-h proestrus phase, when vaginal cytology exhibits only round and nucleated epithelial cells. In nocturnal animals such as rats, early proestrus typically occurs in the morning of the proestrus phase (Becker et al. 2002). Age at recording ranged from P70 to P85. All animals were housed in a temperature- and light-controlled room (23°C, 40% humidity, 12:12-h light-dark cycle) at the Biological Resource Facility of North Carolina State University. All cages were polysulfone bisphenol A (BPA) free and were filled with bedding manufactured from virgin hardwood chips (Beta Chip; NEPCO, Warrensburg, NY) to avoid the presence of endocrine disruptors in corncob bedding (Mani et al. 2005; Markaverich et al. 2002; Villalon Landeros et al. 2012). Soy protein-free rodent chow (2020X; Teklad, Madison, WI) and glass bottle-provided water were available ad libitum.

Animals were divided into two groups to capture late proestrus and to control for a possible circadian cycle effect. One group of animals ($n = 6$) was exposed to a reverse light cycle with lights on at 7:00 PM and off at 7:00 AM, and the other group ($n = 6$) was exposed to a regular light cycle with lights turning on and off at 7:00 AM and 7:00 PM, respectively, as in our previous studies on the effects of the estrous cycle on rat AcbC and caudate-putamen (Proaño et al. 2018, 2019). Estrous cycle assessment was performed beginning on P65 with a wet mount preparation as previously described (Hubscher et al. 2005; Proaño et al. 2018). Females were vaginally swabbed 30 min before lights out, at ~6:30 AM or ~6:30 PM, respectively. Slides were visualized under a microscope to determine estrous cycle stage. No statistically significant differences were detected between animals on a regular light cycle and those on a reverse light cycle. Thus all data from late proestrus are grouped for the remainder of the article. Electrophysiological data from animals in early proestrus were collected from animals experiencing a regular light cycle and were previously published as described above.

Hormone Extractions and Assays

At euthanasia, trunk blood was collected and centrifuged (within 30 min) at 4,000 revolutions/min for 35 min to obtain serum from 33 animals (diestrus: $n = 10$; early proestrus: $n = 7$; late proestrus: $n = 12$; estrus: $n = 4$). Serum was not available from 5 animals (diestrus: $n = 1$; early proestrus: $n = 1$; estrus: $n = 3$). Thus electrophysiology data obtained from these animals was excluded from correlations analysis. Serum was stored at −80°C until extraction. All serum was assayed at the same time. Hormone extraction and enzyme-linked immunosorbent assay protocols were modified from previously described protocols (Chao et al. 2011; Hedges et al. 2018; Krentzel et al. 2020; Tuscher et al. 2016). Briefly, 250 μL of serum were extracted twice with a 10:1 ratio of diethyl ether followed by snap freeze with liquid nitrogen. The ether-containing organic compounds were poured

Table 1. *Circulating levels of estradiol and progesterone across the estrous cycle*

Hormone	Diestrus	Early Proestrus	Late Proestrus	Estrus	Statistics (*F, P*)
17β-Estradiol, pg/mL	8.2 ± 1.3 (10)	11.4 ± 1.7 (7)	11.7 ± 1.6 (12)	8.2 ± 2.3 (4)	1.409, 0.269
Progesterone, ng/mL	**34.8 ± 4.8** (10)[a]	**28.6 ± 7.3** (7)[a]	**51.3 ± 6.1** (12)[b]	**43.4 ± 6.0** (4)[a,b]	**3.173, 0.043**

Values are means ± SE for numbers of animals in parentheses. Boldface indicates statistical significance. [a,b]Superscript letters indicate statistically significant differences across groups. Data were analyzed using a one-way Brown–Forsythe ANOVA.

off into clean glass tubes and dried overnight. This process was conducted twice. Once dry, the samples were resuspended in 200 μL of buffer from the enzyme-linked immunosorbent assay kit (Calbiochem estradiol and Cayman progesterone ELISA kits). Samples were measured in duplicates including extraction efficiency controls. Estradiol and progesterone were measured from the same samples. A 1:100 dilution of the sample was used for the progesterone assay, and the remaining volume of the sample was used for the estradiol assay. Dilution factors were selected based on a dilution curve conducted before the experimental assay. Extraction efficiency for estradiol was 125% with blank at (2.840 ± 0.271 pg/mL, mean ± SE), and intra-assay variability was 14.45%; progesterone measurements were from same extracted samples as estradiol, and therefore they share the same extraction efficiency. Progesterone blank was at (85.365 ± 28.568 pg/mL), and intra-assay variability was 3.3%. All samples were above detectability for the assay. We note that although both employed ELISA kits are advertised by the manufacturers as being able to detect hormone levels in unextracted serum, our experience is that detection levels are substantially decreased when unextracted serum is used. Progesterone levels significantly differed between estrous cycle phases (Table 1). Estradiol levels did not significantly differ (Table 1).

Acute Brain Slice Preparation

Brain slices containing the nucleus accumbens core were prepared as previously described (Proaño et al. 2018). Animals were deeply anesthetized with isoflurane gas before decapitation (~7:00 AM or ~7:00 PM for the reverse and regular light cycles, respectively; for the late proestrus phase that is new to this study). The brain was rapidly extracted into ice-cold oxygenated sucrose artificial cerebrospinal fluid (ACSF) containing (in mM) 75 sucrose, 1.25 NaH_2PO_4, 3 $MgCl_2$, 0.5 $CaCl_2$, 2.4 Na pyruvate, and 1.3 ascorbic acid from Sigma-Aldrich (St. Louis, MO) and 75 NaCl, 25 $NaHCO_3$, 15 dextrose, and 2 KCl from Fisher (Pittsburgh, PA). The osmolarity of the sucrose ACSF was 295–305 mosM, and the pH was between 7.2 and 7.4. Coronal brain slices (300 μm) were prepared with a vibratome and then incubated in regular ACSF containing (in mM) 126 NaCl, 26 $NaHCO_3$, 10 dextrose, 3 KCl, 1.25 NaH_2PO_4, 1 $MgCl_2$, and 2 $CaCl_2$ (295–305 mosM, pH 7.2–7.4) for 30 min at 30–35°C and then for at least 30 min at room temperature (22–23°C). Slices were stored submerged in room-temperature oxygenated ACSF for up to 6 h after sectioning in a large-volume bath holder.

Electrophysiological Recordings

Slices rested for at least 1 h after sectioning. They were then placed in a Zeiss Axioscope equipped with infrared-differential interference contrast (IR-DIC) optics, a Dage IR-1000 video camera, and ×10 and ×40 lenses with optical zoom and superfused with oxygenated ACSF heated to ~21.63°C. Whole cell patch-clamp recordings were used to record the electrical properties of MSNs in the nucleus accumbens core (Fig. 1). MSN density and nucleus accumbens core volume do not differ by sex (Meitzen et al. 2011; Wong et al. 2016). Glass electrodes contained (in mM) 115 K D-gluconate, 8 NaCl, 2 EGTA, 2 $MgCl_2$, 2 MgATP, 0.3 NaGTP, and 10 phosphocreatine from Sigma-Aldrich and 10 HEPES from Fisher (285 mosM, pH 7.2–7.4). Signals were amplified, filtered (2 kHz), and digitized (10 kHz) with a

MultiClamp 700B amplifier attached to a Digidata 1550 system and a personal computer using pCLAMP 10.7 software. Membrane potentials were corrected for a calculated liquid junction potential of 13.5 mV. As previously described (Dorris et al. 2015), recordings were first made in current clamp to assess neuronal electrophysiological properties. MSNs were identified by medium-sized somas, the presence of a slow-ramping subthreshold depolarization in response to low-magnitude positive current injections, a hyperpolarized resting potential more negative than −65 mV, inward rectification, and prominent spike afterhyperpolarization (Belleau and Warren 2000; O'Donnell and Grace 1993). In a subset of recordings, oxygenated ACSF containing both the $GABA_A$ receptor antagonist picrotoxin (PTX, 150 μM; Fisher) and the voltage-gated sodium channel blocker tetrodotoxin (TTX, 1 μM; Abcam Biochemicals) was applied to the bath to abolish inhibitory postsynaptic current events and action potentials, respectively. Once depolarizing current injection no longer generated an action potential, MSNs were voltage clamped at −70 mV and miniature excitatory postsynaptic currents (mEPSCs) were recorded for at least 5 min. These settings enable recordings from almost exclusively AMPA glutamate receptors (Nowak et al. 1984) and were confirmed by our laboratory in a previous study (Proaño et al. 2018), but not in the current study. In all experiments, input/series resistance was monitored for changes, and cells were excluded if resistance changed 25%.

Data Recording and Analysis

Intrinsic electrophysiological properties and action potential characteristics were analyzed with pCLAMP 10.7. After break-in, the resting membrane potential was first allowed to stabilize ~1–2 min, as previously described (Mu et al. 2010). After stabilization, resting membrane potential was assessed in the absence of injected current. At least three series of depolarizing and hyperpolarizing current injections were applied to elicit basic neurophysiological properties. Most properties measured followed definitions previously adopted by our laboratory (Cao et al. 2016; Dorris et al. 2015; Proaño et al. 2018; Willett et al. 2016, 2019), which were based on those of Perkel and colleagues (Farries et al. 2005; Farries and Perkel 2000, 2002; Meitzen et al. 2009). For each neuron, measurements were made of at least
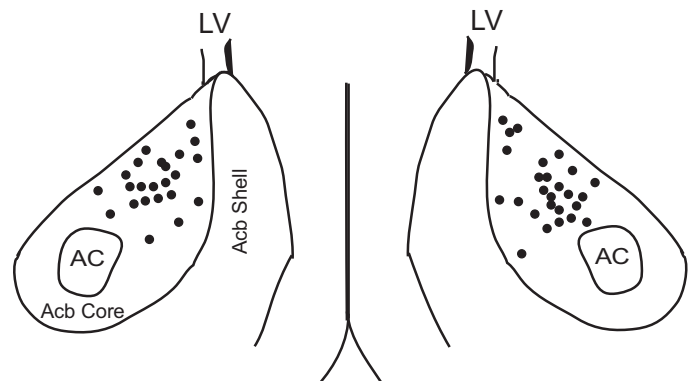

Fig. 1. Location of late proestrus whole cell patch-clamped medium spiny neurons (MSNs) in rat nucleus accumbens core (AcbC). Acb, nucleus accumbens; AC, anterior commissure; LV, lateral ventricle.

three action potentials generated from minimal current injections. These measurements were then averaged to generate the reported action potential measurement for that neuron. For action potential measurements, only the first generated action potential was used unless more action potentials were required to meet the standard three action potentials per neuron. Action potential threshold was defined as the first point of sustained positive acceleration of voltage ($\delta^2 V/\delta t^2$) that was also 3 times the SD of membrane noise before the detected threshold (Baufreton et al. 2005). The delay to first action potential is the average time in milliseconds of the time from the initial deflection generated by the current step function to the action potential threshold of the first spike. Action potential width at half peak is the width of the action potential halfway between action potential peak and threshold in milliseconds. The action potential amplitude is the change in millivolts between action potential threshold and peak. Afterhyperpolarization peak amplitude is the difference in millivolts between action potential threshold and the most hyperpolarized voltage point after action potential peak. Afterhyperpolarization time to peak amplitude is the time measured in milliseconds between the action potential threshold voltage point on the descending phase of the action potential and the afterhyperpolarization peak amplitude. Rheobase, measured in nanoamps, is the lowest amplitude of injected positive current needed to produce an initial action potential. The slope of the linear range of the evoked action potential firing rate-to-positive injected current curve (FI slope) was calculated from the first current stimulus that evoked an action potential to the first current stimulus that generated an evoked firing rate that persisted for at least two consecutive current stimuli. Input resistance in the linear, nonrectified range was calculated from the steady-state membrane potential in response to 0.02-nA hyperpolarizing pulses. Rectified range input resistance, inward rectification, and percent inward rectification were calculated as described previously, with rectified range input resistance measured using the most hyperpolarizing current injected into the MSN (Belleau and Warren 2000). Inward rectification is the input resistance of the 0.02-nA step minus the rectified range input resistance. Percent inward rectification is defined as rectified range input resistance/input resistance $\times$ 100. The time constant of the membrane was calculated by fitting a single exponential curve to the membrane potential change in response to 0.02-nA hyperpolarizing pulses. Possible differences in hyperpolarization-induced "sag" were assessed with the "sag index" (Farries et al. 2005). Briefly, the sag index is defined as the difference between the minimum voltage measured during the largest hyperpolarizing current pulse and the steady-state voltage deflection of that pulse, divided by the steady-state voltage deflection. A cell with no sag would exhibit a sag index of 0, whereas a cell whose maximum voltage deflection is twice that of the steady-state deflection would exhibit a sag index of 1. Cells with considerable sag typically have an index of 0.1. Frequency, amplitude, and decay of mEPSCs were analyzed off-line with Mini Analysis (Synaptosoft, http://www.synaptosoft.com/MiniAnalysis/). mEPSC threshold was set at a minimum value of 5 pA, and accurate event detection was validated by visual inspection. mEPSC frequency was defined as the number of detected mEPSC events per second (Hz). mEPSC amplitude was calculated as the difference between the averaged baseline 10 ms before initial mEPSC rise and peak mEPSC amplitude. mEPSC decay was calculated as the time required for peak mEPSC amplitude to return to baseline.

Statistics

Electrophysiological data were analyzed with a one-way ANOVA with Newman–Keuls post hoc tests, linear regression (Pearson's), and multiple linear regression (GraphPad Prism 8). Hormone concentrations were analyzed using a one-way Brown–Forsythe ANOVA with one-tailed t tests with Welch's correction post hoc tests to control for populations with unequal variances that exhibit skew (GraphPad Prism 8), as previously documented (Krentzel et al. 2020). P values

<0.05 were considered a priori as significant. Data are presented as means $\pm$ SE.

RESULTS

Here we test the central hypothesis that the electrophysiological properties of female rat AcbC MSNs correlate with circulating estradiol, progesterone, or both hormones. Our previously published study on estrous cycle effects on AcbC MSN electrophysiology was originally designed to solely capture early proestrus (Proaño et al. 2018). However, to understand the individual contribution of estradiol and progesterone in modulating MSN electrophysiology, it was necessary to record and characterize electrophysiological properties of MSNs in late proestrus, as well. Thus the results are presented in two parts. *Part I:Late Proestrus* presents a novel characterization of late proestrus AcbC MSN excitatory synapse and intrinsic excitability properties. These data are then combined with the previous data set mentioned above to comprehensively analyze how MSN electrophysiological properties are modulated across the entire estrous cycle (Table 2). With the use of these data, *Part II: Circulating Estradiol and Progesterone Levels, and MSN Electrophysiology* then tests the hypotheses that circulating levels of estradiol, progesterone, and both estradiol and progesterone correlate with specific MSN electrophysiological properties.

Part I: Late Proestrus

mEPSC frequency is drastically decreased in late proestrus. To assess mEPSC properties we voltage clamped MSNs to -70 mV and applied 1 μM TTX and 150 μM PTX solution to block sodium-dependent action potentials and GABA$_A$ receptors, respectively (Fig. 2*A*). We assessed mEPSC frequency, amplitude, and decay (Table 2). mEPSC frequency (Fig. 2*B*) levels were remarkably low, ranging from ~0 to 1 Hz. mEPSC amplitude (Fig. 2*C*) values ranged from around 10 to 22 pA, while mEPSC decay (Fig. 2*D*) levels averaged ~5 ms. When compared with a previous description from other stages of the estrous cycle (Proaño et al. 2018), these findings demonstrate that excitatory synapse properties in late proestrus MSNs show a drastic reduction in mEPSC frequency with a relatively robust increase in amplitude for the existing mEPSC events.

Membrane excitability and passive membrane properties in late proestrus. We also assessed intrinsic electrophysiological properties in late proestrus MSNs, including individual action potential properties, excitability, and passive membrane properties. To accomplish this, we injected MSNs with a series of depolarizing and hyperpolarizing current injections, after which we analyzed an array of electrophysiological attributes. All electrophysiological attributes and related statistical information are provided in Table 2. Here we highlight excitability and passive membrane properties. Membrane excitability was assessed by injecting a series of depolarizing current injections into individual MSNs to quantify action potential initiation and propagation (Fig. 3*A*). We first plotted the number of action potentials evoked by depolarizing current injection curve (FI curve) for individual MSNs (Fig. 3*B*). Using these data, we quantified individual MSN excitability by calculating the slope of the evoked firing rate to positive current curve (FI slope; Fig. 3*C*). We also assessed rheobase, which is the minimum amount of current required to initiate an action potential (Fig.

Table 2. *Nucleus accumbens core medium spiny neuron electrophysiological properties*

Property	Diestrus	Early Proestrus	Late Proestrus	Estrus	Statistics (*F, P*)
mEPSC frequency, Hz	**1.0 ± 0.2** (19)[a]	**2.1 ± 0.4** (12)[b]	**0.4 ± 0.1** (25)[c]	**2.3 ± 0.4** (14)[b]	**12.75, <0.0001**
mEPSC amplitude, pA	**10.4 ± 0.7** (19)[a]	**11.40 ± 0.9** (12)[a]	**15.8 ± 0.5** (25)[b]	**9.1 ± 0.3** (14)[a]	**28.36, <0.0001**
mEPSC decay, ms	**4.2 ± 0.5** (19)[a]	**4.8 ± 0.5** (12)[a]	**3.7 ± 0.2** (25)[a]	**2.7 ± 0.3** (14)[b]	**4.35, 0.0074**
Resting membrane potential, mV	**−83.8 ± 1.1** (26)[b]	**−87.4 ± 0.9** (20)[a]	**−88.2 ± 0.4** (49)[a]	**−88.1 ± 1.5** (16)[a]	**6.40, 0.0005**
Input resistance, MΩ	**299.1 ± 18.7** (26)[a]	**203.9 ± 16.0** (20)[b,c]	**209.4 ± 8.4** (49)[b,c]	**258.6 ± 29.4** (16)[a,b]	**8.53, <0.0001**
Rectified range input resistance, MΩ	**217.5 ± 12.7** (26)[a]	**164.8 ± 12.6** (20)[b,c]	**169.5 ± 6.4** (49)[b,c]	**189.5 ± 17.9** (16)[a,b]	**4.95, 0.003**
Inward rectification, MΩ	**81.7 ± 14.1** (26)[a]	**39.0 ± 5.9** (20)[b,c]	**39.9 ± 3.8** (49)[b,d]	**69.1 ± 19.0** (16)[a,b]	**5.13, 0.002**
Percent inward rectification, %	74.9 ± 3.0 (26)	81.4 ± 2.0 (20)	81.6 ± 1.2 (49)	77.9 ± 4.1 (16)	2.03, 0.115
Sag index (unitless)	0.004 ± 0.004 (26)	0.003 ± 0.001 (20)	0.010 ± 0.002 (49)	0.005 ± 0.004 (16)	1.51, 0.216
Time constant of the membrane, ms	**19.1 ± 1.4** (26)[a]	**14.8 ± 1.2** (20)[a,b]	**13.8 ± 0.7** (49)[b,c]	**16.4 ± 2.4** (16)[a,b,c]	**4.05, 0.009**
Capacitance, pF	68.1 ± 6.1 (26)	78.1 ± 7.4 (20)	68.8 ± 3.4 (49)	65.4 ± 6.4 (16)	0.78, 0.505
Rheobase, pA	**0.1 ± 0.01** (26)[a]	**0.1 ± 0.01** (19)[b]	**0.1 ± 0.01** (49)[b]	**0.1 ± 0.01** (16)[b]	**6.58, 0.0004**
Delay to first AP, ms	**402.3 ± 15.6** (18)[a]	**438.9 ± 13.2** (18)[a,c]	**441.4 ± 9.3** (48)[a,c]	**465.9 ± 14.6** (15)[b,c]	**3.03, 0.033**
AP threshold, mV	−51.8 ± 1.9 (26)	−47.4 ± 2.0 (19)	−47.4 ± 1.0 (49)	−50.5 ± 2.0 (16)	2.06, 0.110
AP amplitude, mV	54.8 ± 3.0 (26)	54.6 ± 3.5 (19)	48.3 ± 1.6 (49)	55.0 ± 3.5 (16)	2.18, 0.095
AP width at half-peak amplitude, ms	**3.8 ± 0.2** (26)[a]	**3.4 ± 0.1** (17)[a]	**4.0 ± 0.1** (49)[b]	**3.6 ± 0.2** (16)[a,b]	**3.80, 0.013**
AHP peak amplitude, mV	**−7.2 ± 0.5** (25)[a]	**−7.7 ± 0.6** (19)	**−9.0 ± 0.4** (49)	**−7.1 ± 0.5** (16)	**3.97, 0.010**
AHP time to peak, ms	25.8 ± 3.1 (25)	23.2 ± 2.1 (19)	25.7 ± 1.5 (49)	26.3 ± 3.3 (16)	0.26, 0.854
FI slope, Hz/nA	**298.7 ± 17.9** (26)[a]	**241.3 ± 14.8** (19)[b]	**238.5 ± 7.1** (49)[b]	**297.1 ± 21.2** (16)[a]	**6.22, 0.001**

Excitatory synaptic input and intrinsic excitability properties recorded from diestrus, early and late proestrus, and estrus medium spiny neurons in gonad-intact adult rat nucleus accumbens core. Values are means ± SE for numbers of animals in parentheses. Boldface indicates statistical significance. [a,b,c,d]Superscript letters indicate statistically significant differences across groups. Data were analyzed with a one-way ANOVA with Newman–Keuls post hoc tests. AHP, afterhyperpolarization; AP, action potential; FI, evoked firing rate-to-positive current curve.

3*D*). Regarding passive membrane properties, a series of hyperpolarizing current injections were administered to MSNSs (Fig. 4*A*). A plot of the steady-state voltage deflection evoked by injected hyperpolarizing current curve (IV curve; Fig. 4*B*) reveals inward rectification, as expected from previous studies of MSNs (Belleau and Warren 2000). We then quantified input resistance in the linear (Fig. 4*C*) and rectified ranges (Fig. 4*D*). These findings indicate that the excitability and passive membrane properties of late proestrus MSNs fall within an expected range from previous studies except for mEPSC frequency. As a whole, these data enable a more complete analysis of AcbC MSN properties across the estrous cycle (Table 2).

Part II: Circulating Estradiol and Progesterone Levels, and MSN Electrophysiology

The rat estrous cycle features cyclical fluctuations of estradiol and progesterone over a 4- to 5-day period. It can be divided into multiple phases, including the diestrus, early and late proestrus, and estrus phases. Our previous study demonstrated robust changes in adult female AcbC MSN electrophysiological properties across the estrous cycle, which were abolished upon gonadectomy (Proaño et al. 2018). Our previous study did not analyze whether the electrophysiological properties of MSNs varied with circulating levels of estradiol or progesterone. This is notable gap in knowledge, as answering this question may provide clues toward the underlying endocrine mechanisms. Thus here we tested the hypothesis that circulating levels of estradiol, progesterone, and both estradiol and progesterone correlate with specific MSN electrophysiological properties.

Circulating estradiol levels correlate with resting membrane potential, the time constant of the membrane, and rheobase. To test the hypothesis that circulating levels of estradiol correlate with specific MSN electrophysiological properties, we tested whether each animal's circulating estradiol levels correlated with all the MSN properties collected across all phases of the

estrous cycle. Three electrophysiological properties significantly correlate with circulating estradiol levels: resting membrane potential, the time constant of the membrane, and rheobase. Complete statistical information is provided in Tables 2 and 3. Resting membrane potential exhibited an inverse correlation with increasing circulating levels of estradiol across the estrous cycle (Fig. 5*A*), suggesting that as estradiol levels increase, resting membrane potential decreases. If this relationship is robust, then the estrous cycle phases that feature higher circulating estradiol levels would exhibit hyperpolarized resting membrane potentials. Supporting this, resting membrane potential was significantly hyperpolarized in both early and late proestrus compared with the diestrus phase (Fig. 5*B*). Interestingly, resting membrane potential remained hyperpolarized in the estrus phase compared with the diestrus phase, even though circulating levels of estradiol are decreasing in this phase. This may indicate that MSNs have yet to revert to a non-estradiol-influenced state, as well as a potential role for a synergistic interaction between estradiol and progesterone, which is addressed below. The time constant of the membrane exhibited an inverse correlation with increasing levels of circulating estradiol (Fig. 5*C*), suggesting that as estradiol levels increase, the time constant of the membrane decreases. To support this, the time constant of the membrane decreased during late proestrus phase compared with the diestrus phase (Fig. 5*D*). Rheobase featured a positive correlation with increasing circulating estradiol levels (Fig. 5*E*). This finding indicates that the minimum amount of current required to initiate the first action potential increases as circulating levels of estradiol increase. If this correlation is robust, then we would expect that the estrous cycle phases that feature higher circulating estradiol levels would exhibit increased rheobase values. Consistent with this logic, rheobase was significantly elevated in early and late proestrus compared with the diestrus phase (Fig. 5*F*). Rheobase was also significantly increased in the estrus phase compared with the diestrus phase, again
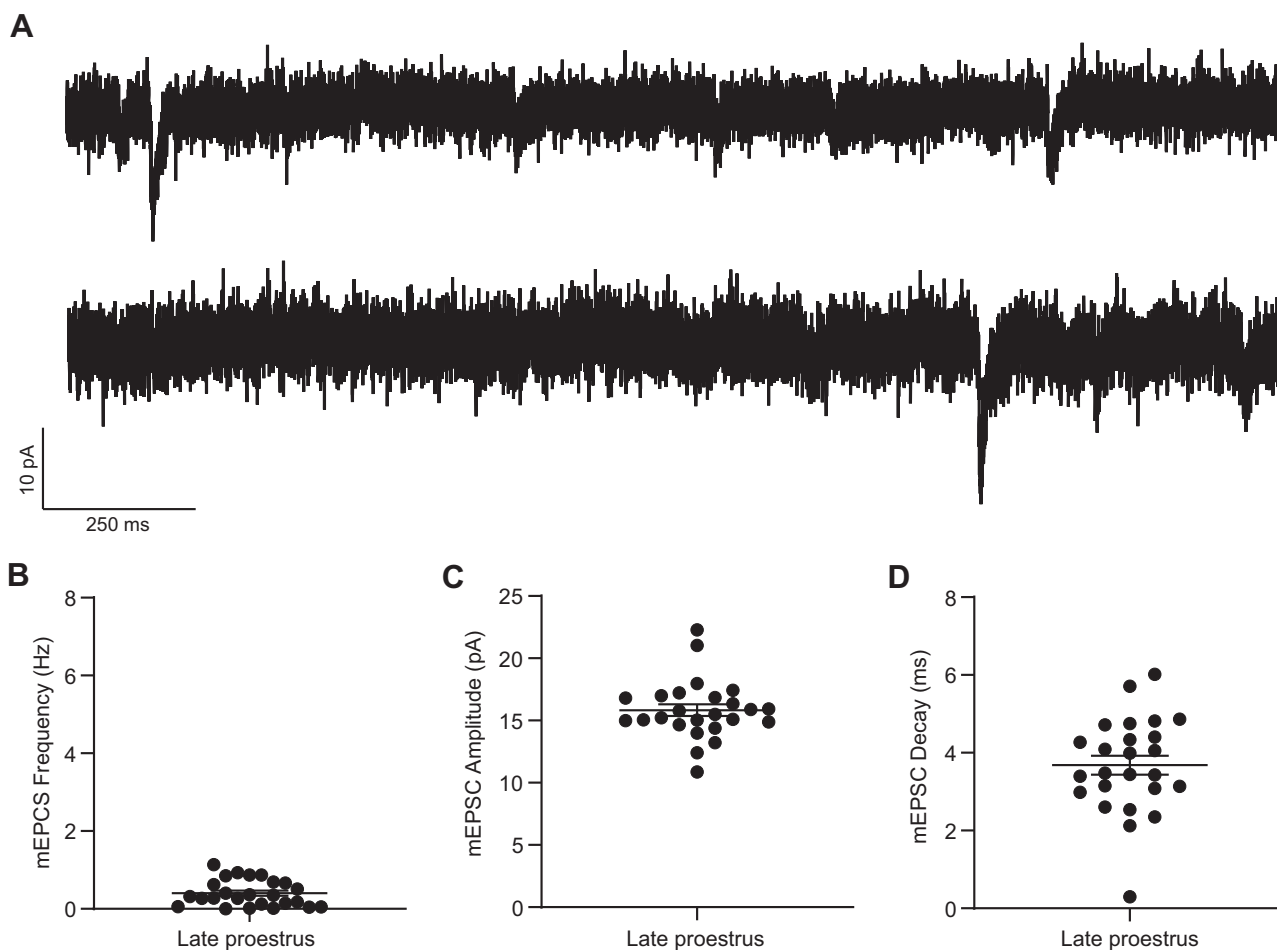
Fig. 2. Medium spiny neuron (MSN) miniature excitatory postsynaptic current (mEPSC) properties from late proestrus females. *A*: representative examples of mEPSCs recorded in late proestrus. *B*: mEPSC frequency. *C*: mEPSC amplitude. *D*: mEPSC decay. Horizontal line superimposed on scatterplots in *B–D* indicates the mean. Complete statistical information is in Table 2.

suggesting a possible remaining impact of estradiol. Overall, these findings indicate that circulating levels of estradiol associate with resting membrane potential and rheobase. The association between estradiol, resting membrane potential, and rheobase is logical given that a more hyperpolarized resting membrane potential would require increasing rheobase values to drive the neuron toward threshold and fire an action potential. Thus increasing circulating estradiol levels decrease the overall intrinsic excitability of AcbC MSNs.

Circulating progesterone levels correlate with mEPSC frequency and mEPSC amplitude. To test the hypothesis that circulating levels of progesterone correlate with specific MSN electrophysiological properties, we tested whether each animal's circulating progesterone levels correlated with all the MSN properties collected across all phases of the estrous cycle. Two electrophysiological properties significantly correlated with circulating progesterone levels: mEPSC frequency and mEPSC amplitude. Complete statistical information is provided in Tables 2 and 3. mEPSC frequency exhibited an inverse correlation with increasing circulating levels of progesterone (Fig. 6*A*). This finding indicates that mEPSC frequency decreases as progesterone levels increase. If this correlation is robust, then we would expect that the estrous cycle phases that feature higher circulating levels of progesterone would exhibit a decrease in mEPSC frequency. Consistent with

this rationale, mEPSC frequency was significantly decreased in late proestrus compared with early proestrus and estrus phases (Fig. 6*B*). Interestingly, mEPSC frequency rebounded during the estrus phase, suggesting a possible acute effect of progesterone or estradiol. mEPSC amplitude featured a positive correlation with increasing circulating levels of progesterone (Fig. 6*C*), indicating that mEPSC amplitude increases as progesterone levels increase. If this is a robust correlation, then we would expect that estrous cycle phases that feature higher circulating progesterone levels would exhibit increased mEPSC amplitude. Consistent with this, mEPSC amplitude was significantly increased in late proestrus compared with the diestrus, early proestrus, and estrus phases of the cycle (Fig. 6*D*). Interestingly, the variance of mEPSC amplitude values decreased radically during the estrus phase, suggesting a potential synergistic action between estradiol and progesterone. Overall, this analysis indicates that increasing circulating levels of progesterone alter MSN excitatory synapse properties.

Circulating estradiol and progesterone levels together correlate with mEPSC amplitude, resting membrane potential, input resistance, and rectified range input resistance. To test the hypothesis that circulating levels of estradiol and progesterone together correlate with specific MSN electrophysiological properties, we tested whether each animal's circulating estradiol and progesterone levels correlate with all the MSN
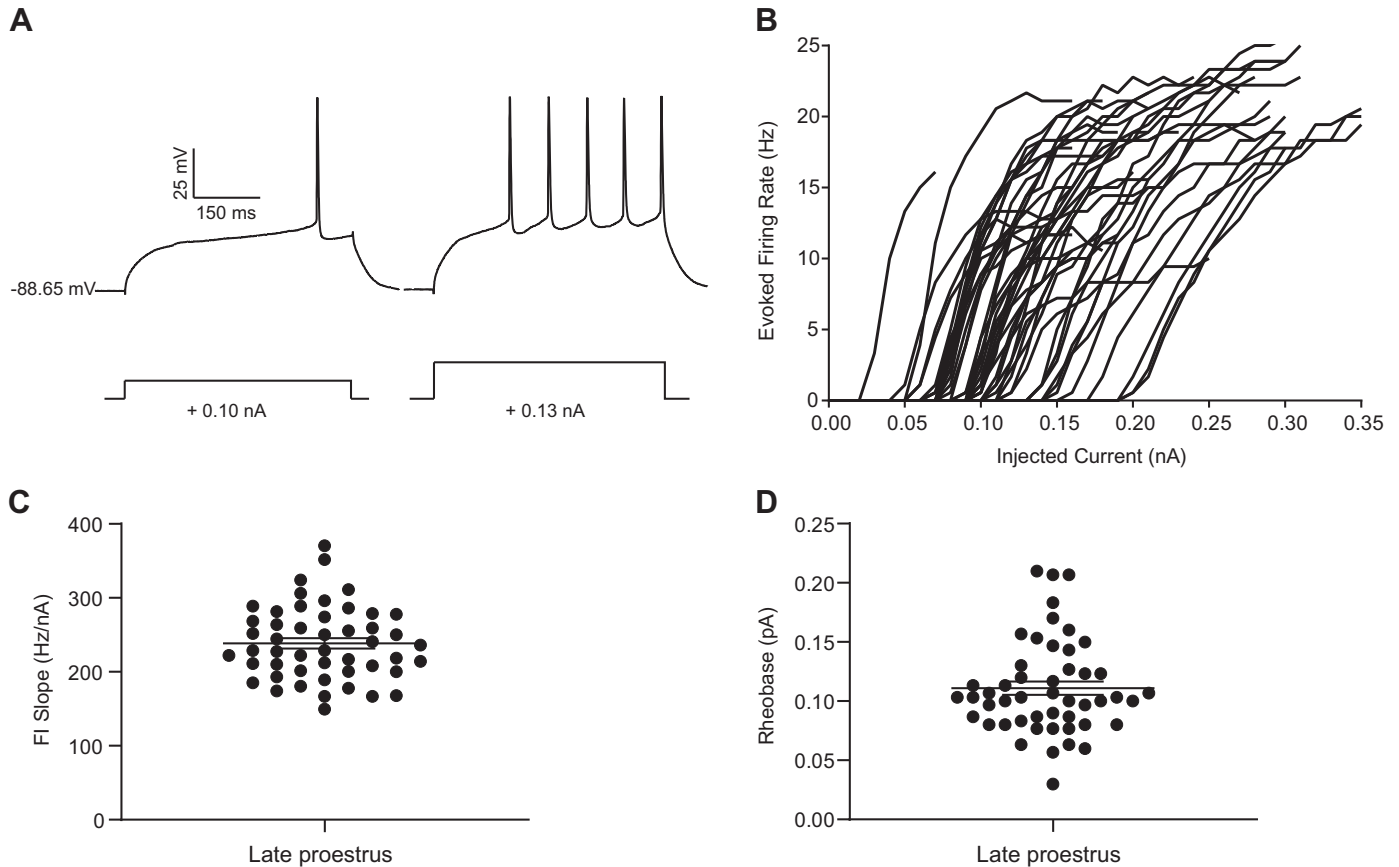
Fig. 3. Medium spiny neuron (MSN) action potential initiation and propagation properties in late proestrus females. *A*: voltage response of late proestrus female MSNs to a series of depolarizing current injections. *B*: action potential firing rates evoked by depolarizing current injections. *C*: slopes of the evoked firing rate-to-positive current curve (FI slope) in individual MSNs. *D*: rheobase. Horizontal line superimposed on scatterplots in *C* and *D* indicates the mean. Complete statistical information is in Table 2.

properties collected across all phases of the estrous cycle using a multiple linear regression with estradiol and progesterone as two independent variables. Four electrophysiological properties significantly correlated with circulating estradiol and progesterone levels: resting membrane potential, input resistance, rectified range input resistance, and mEPSC amplitude. Complete statistical information is provided in Tables 2 and 3. Resting membrane potential correlates with the interaction between circulating levels of estradiol and progesterone. Consistent with this finding, resting membrane potential remained hyperpolarized in late proestrus and estrus phases compared with the diestrus phase, when the effects of both estradiol and progesterone would potentially manifest (Fig. 5*B*). Input resistance in the linear range correlated with the interaction between circulating levels of estradiol and progesterone. Supporting this finding, input resistance was significantly lower in early and late proestrus compared with the diestrus phase, with intermediate values in the estrus phase (Fig. 7*A*). Input resistance in the rectified range also correlated with the interaction between circulating levels of estradiol and progesterone. Accordingly, rectified range input resistance was significantly decreased in early and late proestrus compared with the diestrus phase, and again exhibited intermediate values in the estrus phase (Fig. 7*B*). mEPSC amplitude also correlated with the interaction between circulating levels of estradiol and progesterone (Table 3). As expected, mEPSC amplitude began to increase in early proestrus when circulating levels of estradiol increase and was

significantly increased in late proestrus when circulating levels of progesterone increase (Fig. 6*C*).

DISCUSSION

The findings presented here demonstrate differential and synergistic roles of estradiol and progesterone in the modulation of AcbC MSN electrophysiological properties across the estrous cycle. Circulating levels of estradiol correlate with resting membrane potential, the time constant of the membrane, and rheobase, while circulating levels of progesterone correlate with mEPSC frequency and amplitude. Furthermore, when analyzed in combination, circulating levels of estradiol and progesterone correlate with mEPSC amplitude, resting membrane potential, and input resistance in both the linear and rectified ranges. These correlations compare with the changes in MSN properties across estrous cycle phases, including the late proestrus phase presented in this study, which features a notable decrease in mEPSC frequency. Collectively, this study provides the first mechanistic clues of the underlying neuroendocrine mechanisms that shape AcbC input-output properties, which bears relevance to the associated changes in AcbC-mediated behaviors and functions across the estrous cycle.

Our previously published data on AcbC properties across the estrous cycle established two competing interpretations for the changes in MSN excitatory synapse and intrinsic excitability properties. One interpretation is that these changing properties
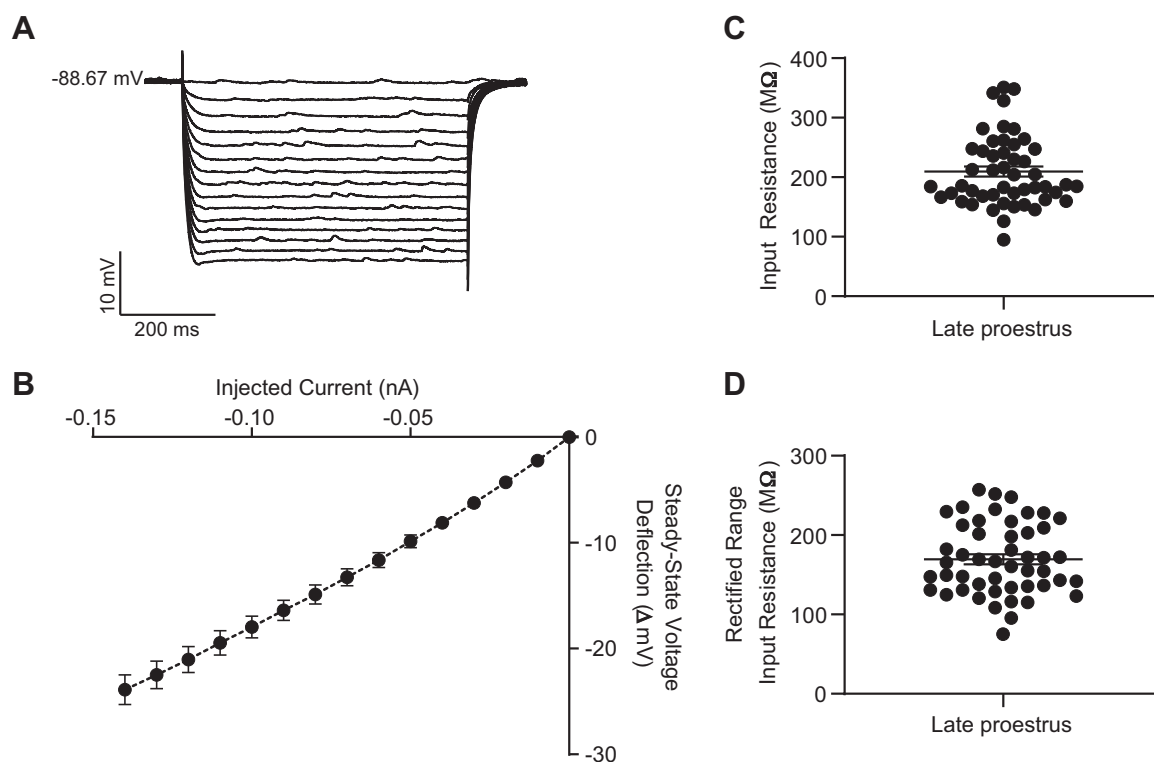
Fig. 4. Medium spiny neuron (MSN) passive electrophysiological properties in late proestrus females. *A*: voltage response of late proestrus female MSNs to a series of hyperpolarizing current injections. *B*: the injected current-to-steady-stage voltage deflection curve (IV curve). *C*: input resistance in the linear range. *D*: input resistance in the rectified range. Horizontal line superimposed on scatterplots in *C* and *D* indicates the mean. Complete statistical information is in Table 2.

directly facilitate changes in AcbC function with resulting impacts on behavior. A second interpretation suggests that changes in excitatory synaptic input and intrinsic excitability compensate for each other. This type of change would mitigate differential circuit output, perhaps via a homeostatic plasticity mechanism (Tien and Kerschensteiner 2018; Turrigiano 2012). This second interpretation is based on potentially contrasting changes in excitatory synapse properties and intrinsic excitability between diestrus MSNs when compared with early proestrus and estrus MSNs. Briefly, MSNs in the diestrus phase demonstrated decreased mEPSC frequency and increased intrinsic excitability compared with early proestrus and estrus phase MSNs. This data set, however, did not include metrics from AcbC MSNs in the late proestrus phase. This omission was notable given that the late proestrus phase of the estrous cycle demonstrates different hormonal, behavioral, and reproductive functions compared with other phases of the cycle. As demonstrated by the current study, the potentially contrasted changes in excitatory synapse properties and intrinsic excitability exhibited between diestrus compared with early proestrus and estrus dissipated during late proestrus (Fig. 8).

These findings indicate that these properties are dissociable, potentially controlled by different hormones, and are likely not a type of homeostatic plasticity. In short, changes in excitatory synaptic input can be disengaged from changes in intrinsic excitability, and vice versa. Another line of evidence arguing against homeostatic plasticity is the heterogeneity in electrophysiological changes and their relationship to circulating levels of either estradiol, progesterone, or the combination of both, as may occur during the estrus phase. Several electro-

physiological properties during the estrus phase assumed a more diestrus-like phenotype, and others assumed a more proestrus-like (both early and late) phenotype, while others acquired more intermediate values. This suggests that specific cellular properties revert to a "non-hormone-influenced" state at different timescales, indicating temporal differentiation as well as divergent mechanism of hormone action and further arguing against the presence of homeostatic synaptic plasticity. Thus we believe that the preponderance of evidence favors the first interpretation: changing electrophysiological properties across the estrous cycle directly facilitate changes in AcbC function.

Intriguingly, circulating levels of estradiol alone correlate with intrinsic excitability but not excitatory synapse properties. Circulating levels of estradiol correlated with resting membrane potential, the time constant of the membrane, and rheobase, which all determine neuronal excitability. If estradiol is acting directly on MSNs and not an afferent target, there are several estrogen receptor types that may be responsible for this action, as the AcbC and other striatal regions express membrane-associated estrogen receptors (mERs) α, β, and GPER-1 with sparse or no expression of nuclear receptors in adult animals (Almey et al. 2012, 2015). We do note that a detailed characterization of estrogen receptor expression across development and estrous cycle phase in the AcbC and afferent regions has not been published. A potential mechanism for changes in membrane excitability properties is through estradiol's action on mERα and mERβ, along with their association with metabotropic glutamate receptors, to induce L-type calcium currents as well as CREB phosphorylation in the striatum

Table 3. *Correlations between estradiol and progesterone with AcbC MSN electrophysiological properties*

Property	Correlations (r, P)		
	Estradiol	Progesterone	Estradiol + Progesterone
mEPSC frequency, Hz	−0.01, 0.93	**−0.30, 0.03**	0.23, 0.10
mEPSC amplitude, pA	0.06, 0.70	**0.35, 0.01**	**0.28, 0.04**
mEPSC decay, ms	−0.001, 0.99	0.08, 0.57	0.07, 0.65
Resting membrane potential, mV	**−0.25, 0.02**	−0.12, 0.28	**0.24, 0.02**
Input resistance, MΩ	−0.20, 0.05	−0.19, 0.08	**0.26, 0.01**
Rectified range input resistance, MΩ	−0.16, 0.12	−0.12, 0.24	**0.22, 0.04**
Inward rectification, MΩ	−0.17, 0.12	−0.18, 0.09	0.20, 0.05
Percent inward rectification, %	0.15, 0.16	0.11, 0.32	0.13, 0.22
Sag index (unitless)	0.03, 0.76	0.04, 0.68	0.05, 0.62
Time constant of the membrane, ms	**−0.21, 0.04**	−0.12, 0.28	0.18, 0.09
Capacitance, pF	0.03, 0.77	0.03, 0.78	0.08, 0.46
Rheobase, pA	**0.28, 0.01**	−0.02, 0.85	0.18, 0.09
Delay to first AP, ms	0.21, 0.06	0.06, 0.60	0.12, 0.27
AP threshold, mV	0.14, 0.18	0.02, 0.84	0.09, 0.38
AP amplitude, mV	0.04, 0.70	−0.06, 0.57	0.03, 0.77
AP width at half-peak amplitude, ms	−0.01, 0.95	−0.01, 0.90	0.01, 0.93
AHP peak amplitude, mV	0.05, 0.64	−0.04, 0.68	0.04, 0.74
AHP time to peak, ms	−0.15, 0.15	−0.09, 0.39	0.16, 0.14
FI slope, Hz/nA	−0.14, 0.20	0.03, 0.76	0.01, 0.35

Relationship between estradiol or progesterone and estradiol plus progesterone with excitatory synaptic input and intrinsic excitability properties of medium spiny neurons (MSNs) in gonad-intact adult rat nucleus accumbens core (AbcC) across the estrous cycle. Boldface indicates statistical significance. Data were analyzed using multiple linear regression. AHP, afterhyperpolarization; AP, action potential; FI, evoked firing rate-to-positive current curve; mEPSC, miniature excitatory postsynaptic current.

(Grove-Strawser et al. 2010; Mermelstein et al. 1996). The lack of a correlation with estradiol and excitatory synapse properties is interesting. One speculative explanation for this is that the primary actions of estradiol on excitatory synapse properties occur after peak estradiol actions are reached, preventing a statistical correlation. Consistent with this explanation, previous studies have found that multiple estradiol injections in female rats change AcbC-associated behaviors as well as dopaminergic and glutamatergic synaptic transmission (Becker and Rudick 1999; Cao et al. 2018; Krentzel et al. 2019, 2020; Miller et al. 2020). Important for excitatory synapse properties, an overall decrease in dendritic spine density was reported in AcbC but not caudate-putamen MSNs (Peterson et al. 2015). In addition, sex differences in excitatory synapse number and associated markers in AcbC MSNs have been identified between proestrus females and males (Forlano and Woolley 2010; Wissman et al. 2012). Inconsistent with this explanation, in adult female but not male AcbC, bath estradiol administration rapidly decreased mEPSC frequency (Krentzel et al. 2019). However, one caveat to the study from Krentzel and colleagues is that it was not designed to detect potential differences across the estrous cycle. We also note that another caveat, for both Krentzel et al. 2019 and the current study, is that MSN subtype was not addressed. It is possible that estradiol and progesterone differentially modulate MSNs depending on the type of dopamine receptor expressed, through either direct or indirect actions via afferent excitatory inputs. Importantly, aromatase may also be present in the striatum (Horvath et al. 1997; Jakab et al. 1993; Tozzi et al. 2015; Wagner and Morrell 1996). Thus it remains possible that both de novo synthesis of estradiol in the striatum and ovarian estradiol can regulate AcbC electrophysiological properties in both acute and longer term time frames. We also note that the nature of the current study, in that it combined new data with a past (although recently and sequentially generated) data set,

generates the possibility of uncontrolled variables, although the principle finding that the estrous cycle modulates MSN electrophysiology was recently replicated by another laboratory in a different experimental context and rat line (Alonso-Caraballo and Ferrario 2019). We note that uncontrolled variables are potentially present even in experiments that collect all experimental groups at the same time. Further mitigating the limitations of this particular study are that the exact same methods and equipment were employed in both studies, as were the same first and last authors. We also searched for a priori expected consistencies in the data sets. For instance, most but not all of the electrophysiological properties between late proestrus and estrus are the same, as would be expected if the data sets were comparable (for example, Fig. 5*B*). Overall, we believe that the scientific advantages generated by combining the two data sets outweigh the limitations documented above.

Collectively, these data indicate that AcbC MSNs may exhibit a specific long-term estradiol sensitivity in intrinsic excitability and an acute estradiol sensitivity in excitatory synapse properties that could be related to the AcbC's role in motivated reproductive behaviors (Tonn Eisinger et al. 2018). These behaviors include, perhaps, rapid changes in sexual receptivity detected during the estrous cycle (Micevych et al. 2017; Yoest et al. 2018), paced mating behavior (Jenkins and Becker 2001), sexual reward (Meisel and Mullins 2006), and locomotor and anxiety-related behaviors (Krentzel and Meitzen 2018; Krentzel et al. 2020; Miller et al. 2020). Importantly, correlation is not causation, and an important future direction of this research will be to establish causal roles of circulating estradiol and progesterone levels via exogenous hormone supplementation of ovariectomized (OVX) females. Future research will also need to determine whether estradiol and progesterone are acting directly on the nucleus accumbens, and whether estradiol and progesterone are acting on different cellular targets.
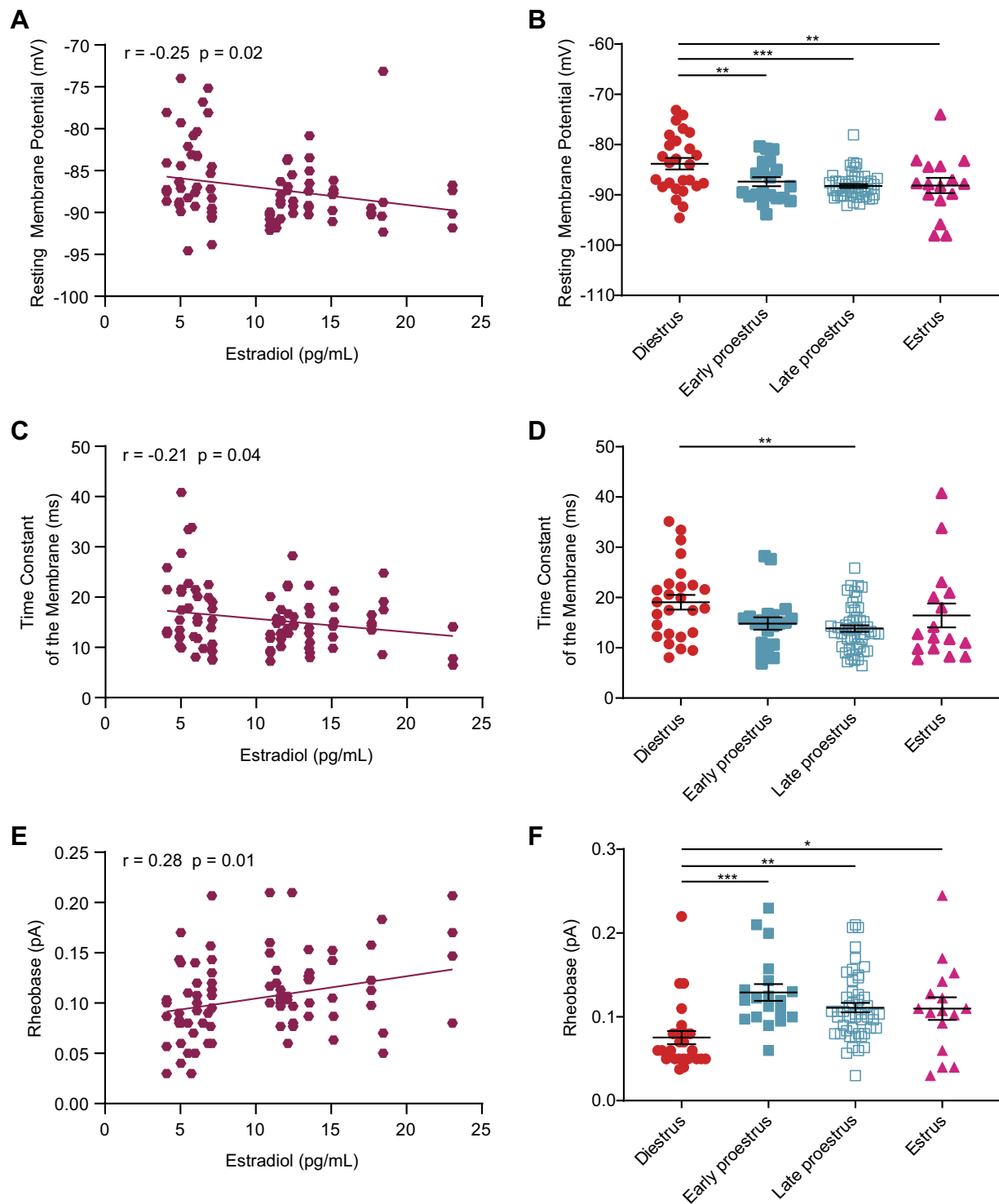
Fig. 5. Correlations of select electrophysiological properties across all phases of the estrous cycle with circulating levels of estradiol. Resting membrane potential (*A*) and time constant of the membrane (*C*) inversely correlate with circulating levels of estradiol. Rheobase (*E*) displays a positive correlation with circulating levels of estradiol. Resting membrane potential (*B*), time constant of the membrane (*D*), and rheobase (*F*) vary across estrous cycle phase. Horizontal line superimposed on scatterplots in *B*, *D*, and *F* indicates the mean. Lines above the scatterplots indicate statistical significance. *$P < 0.05$; **$P < 0.01$; ***$P < 0.001$. Complete statistical information is in Tables 2 and 3.

Although most striatal sex-focused research has concentrated on estradiol (Meitzen et al. 2018; Yoest et al. 2014), progesterone is also an important factor for the estrous cycle, especially for late proestrus and estrus phases. In this study, we found that progesterone correlated with several excitatory syn-

apse properties, including mEPSC frequency and amplitude. Consistent with a possible relationship of progesterone and excitatory synapse properties, mEPSC frequency during late proestrus drastically decreased to levels unrivaled by other estrous cycle phases while maintaining comparable levels of
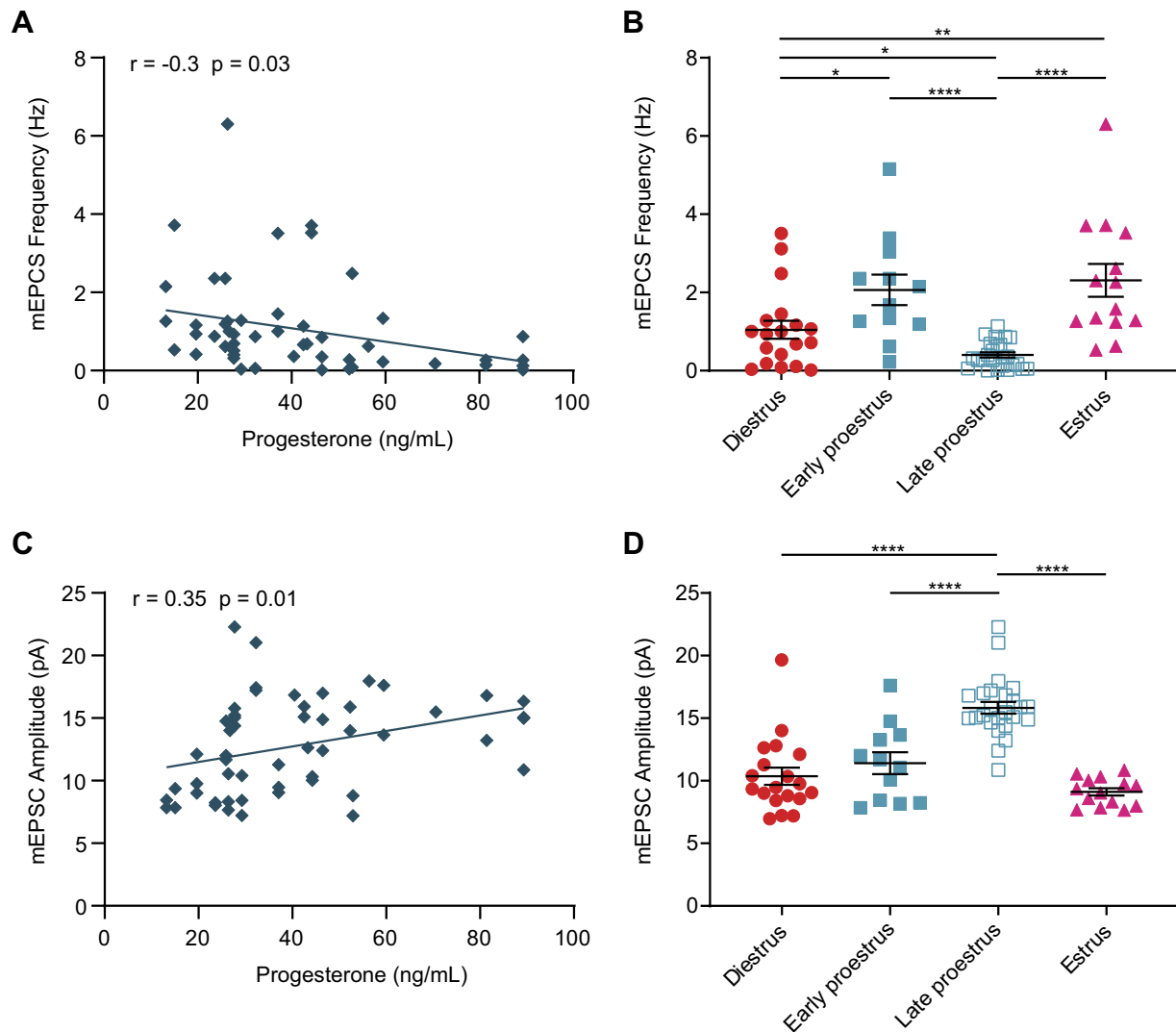
Fig. 6. Correlation of select electrophysiological properties across all phases of the estrous cycle with circulating levels of progesterone. Miniature excitatory postsynaptic current (mEPSC) frequency (*A*) inversely correlates with circulating levels of progesterone. mEPSC amplitude (*C*) shows a positive correlation with circulating levels of progesterone. mEPSC frequency (*B*) and amplitude (*D*) vary across estrous cycle phase. Horizontal line superimposed on scatterplots in *B* and *D* indicates the mean. Lines above the scatterplots indicate statistical significance. *$P < 0.05$; **$P < 0.01$; ****$P < 0.0001$. Complete statistical information is in Tables 2 and 3.

intrinsic excitability to early proestrus and estrus MSNs. This sharp decrease in mEPSC frequency suggests a curtailment in excitatory synaptic properties that might be mediated by an acute effect of progesterone, in addition to the acute action of estradiol discussed above (Krentzel et al. 2019). Regardless of the underlying mechanism, there is precedent for progesterone inducing differences in synapse properties either in the context of the estrous cycle or via exogenous supplementation in ovariectomized animals. Progesterone exposure has been shown to rapidly decrease dendritic spine density in pyramidal neurons in area CA1 of the hippocampus in female rats during the 24-h window between late proestrus and estrus (Woolley- and McEwen 1993). A decrease in dendritic spine density often but not always correlates with a decrease in mEPSC frequency. Thus it is possible that just as in the hippocampus, increasing circulating levels of progesterone in the AcbC during late proestrus may induce the sharp decrease in mEPSC frequency, bearing in mind that this may be one of several mechanisms

that synergistically work to decrease excitatory synapse properties.

Regarding specific progesterone action in the AcbC and other striatal regions, select studies have directly addressed this question. Importantly, evidence for progesterone receptor expression in the striatal regions has been documented in several species that include rodents and birds. Thus here we briefly review relevant evidence for striatal progesterone action. A primary culture study on striatal cells from C57B2/J6 mice detected progesterone receptor encoding mRNA (Piechota et al. 2017). In rats, bovine serum albumin (BSA)-conjugated progesterone bound to striatal cells, demonstrating the presence of membrane-associated progesterone receptors (Dluzen and Ramirez 1989b; Ke and Ramirez 1990). A study in the domestic hen identified AcbC cell nuclei expressing progesterone receptors by using immunohistochemistry (Sterling et al. 1987). In reference to progesterone action in the striatum, a study from 1984 found that progesterone exerted a biphasic
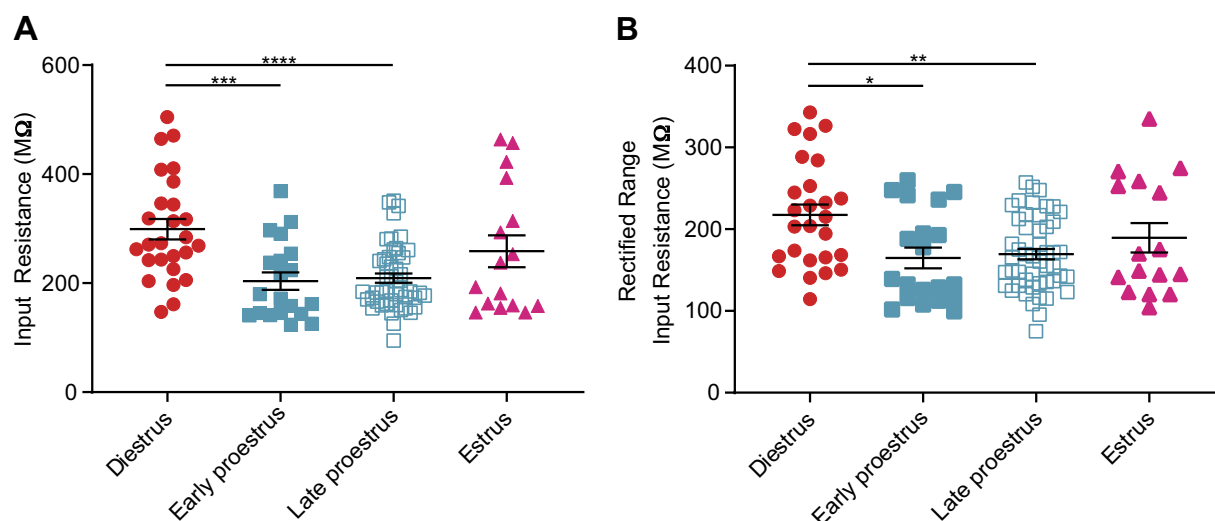
Fig. 7. Correlation of select electrophysiological properties across all phases of the estrous cycle with circulating levels of estradiol and progesterone. Input resistance in the linear range (*A*) and input resistance in the rectified range (*B*) vary across estrous cycle phase. Horizontal line superimposed on scatterplots in *A* and *B* indicates the mean. Lines above the scatterplots indicate statistical significance. *$P < 0.05$; **$P < 0.01$; ***$P < 0.001$; ****$P < 0.0001$. Complete statistical information is in Tables 2 and 3.

effect on dopamine release. Progesterone administration to OVX-estradiol-primed female rats 2 to 12 h before euthanasia potentiated spontaneous- and amphetamine-induced dopamine release, while progesterone administration 24 h before euthanasia largely inhibited the spontaneous- and amphetamine-induced release of dopamine (Dluzen and Ramirez 1984). This difference in temporal action of progesterone is highly suggestive of possible differential temporal actions in the context of the estrous cycle. Another study by the same group found that amphetamine application along with a pulsatile administration of BSA-conjugated progesterone produced maximal levels of dopamine release compared with continuous BSA-conjugated progesterone application or vehicle controls (Dluzen and Ramirez 1989a, 1989b). In a different study, progesterone and *N*-methyl-D-aspartate (NMDA) application onto striatal slices from proestrus female rats amplified the release of dopamine that was normally caused by NMDA administration alone (Cabrera and Navarro 1996). These studies suggest a close interaction between progesterone and glutamatergic systems in the striatum that modulate the release of dopamine, in addition to the well-known role of estradiol. In a pathological context, progesterone has been shown to modulate AcbC-mediated behaviors related to drugs of abuse (Becker 1999). Cocaine-induced place preference behavior was decreased in rats that received an acute dose of progesterone (Russo et al. 2003). In humans, women in the luteal phase of the menstrual cycle, when progesterone levels are high, have a reduced desire to smoke cocaine and an attenuated subjective response to cocaine than during the follicular phase (Evans and Foltin 2006; Sofuoglu et al. 2002), albeit the luteal phase also features moderate levels of estradiol. Finally, in addition to a possible role of progesterone in regulating excitatory synapse, progesterone metabolites such as allopregnanolone have long been documented to act on GABA receptors, which AcbC MSNs also express (Bitran et al. 1995). Collectively, this body of evidence suggests that progesterone may modulate the electrophysiology AcbC MSNs and resulting behaviors.

So far, we have discussed the effects of estradiol and progesterone separately. However, our study also indicates that some electrophysiological properties correlate with estradiol and progesterone in combination. These properties include mEPSC amplitude, resting membrane potential, and input resistance in both the linear and rectified ranges. The combined action of estradiol and progesterone in the regulation of these properties is supported by the dual action of these hormones in proestrus and potential after-actions in estrus (Becker et al. 2002) (Fig. 8). This suggests several possible hormonal mechanisms that may induce the sharp decrease in mEPSC frequency in late proestrus (Fig. 8). All of these possible mechanisms focus on a presynaptic locus of action. This is because the changes in mEPSC frequency are much more robust than changes in mEPSC amplitude. With this stated, we acknowledge that there are potential postsynaptic actions, as well. With regard to presynaptic mechanisms, first, estradiol and progesterone may both decrease mEPSC properties, but via potentially different mechanisms and timeframes. Following an acute decrease in AcbC MSN mEPSC frequency via estradiol (Krentzel et al. 2019), progesterone may also acutely decrease mEPSC frequency, which is a testable hypothesis and can be disproved or confirmed by future experiments. Both hormones may also induce decreases in dendritic spine density, with estradiol and progesterone exposure speeding this decrease as has been show using exogenous exposure to ovariectomized rat hippocampus (McEwen and Woolley 1994; Woolley and McEwen 1993). If this model is accurate, then it predicts that dendritic spine density will be decreased in the AcbC during late proestrus and potentially estrus. It also predicts that, like exogenous estradiol exposure, exogenous progesterone exposure likewise decreases dendritic spine density in AcbC MSNs. This model does not rule out other, synergistic potential mechanisms. One mechanism is a possible association between ovarian hormones and glial cells across the estrous cycle. Data indicate that the number of axosomatic excitatory synapses on neurons in the arcuate nucleus of the hypothalamus begins to decrease during early proestrus, remains low until the morning
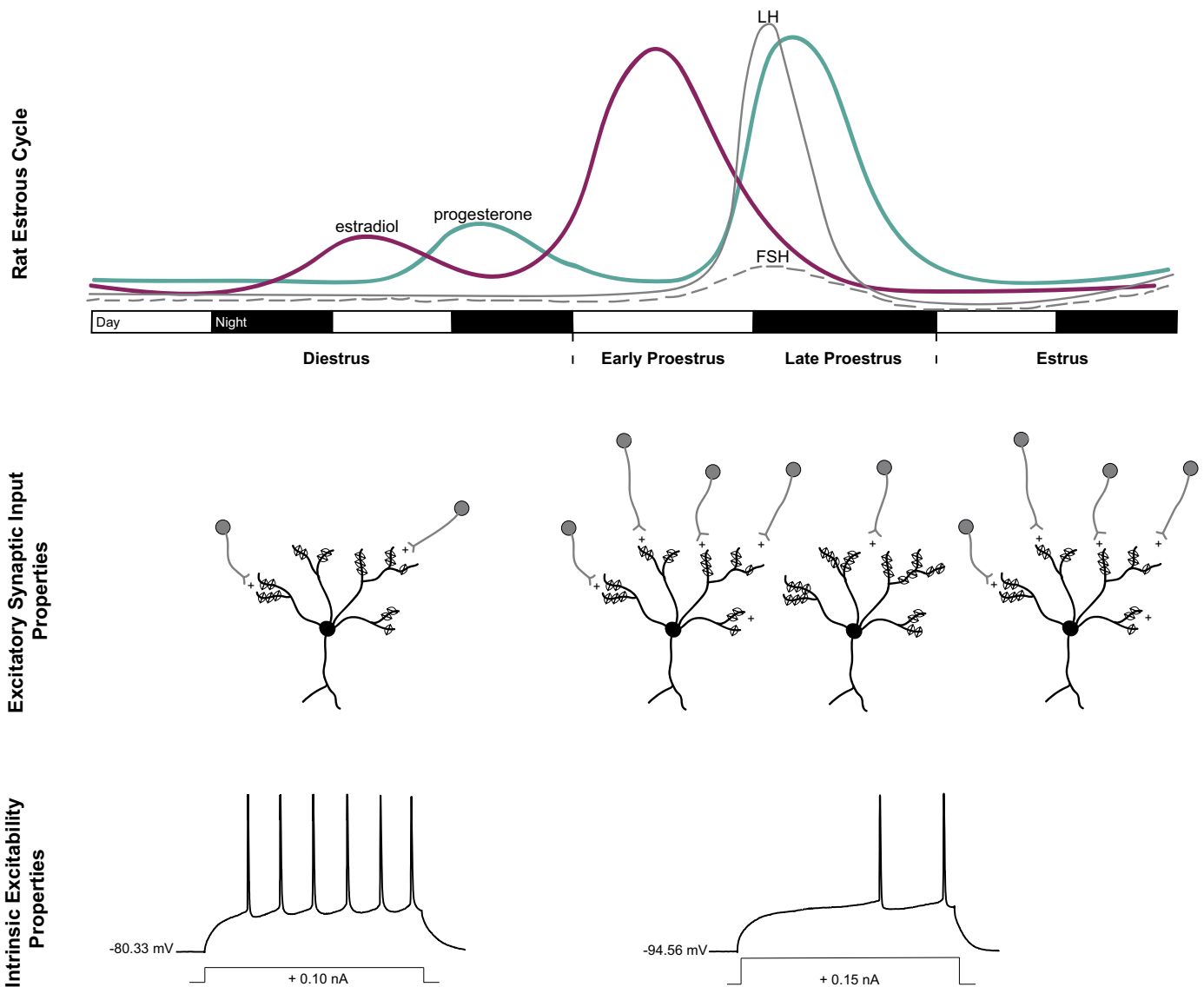
Fig. 8. Schematic of nucleus accumbens core (AcbC) in medium spiny neuron (MSN) excitatory synapse and intrinsic excitability properties between estrous cycle phases in the adult female rat. Excitatory synapse properties are decreased in the diestrus stage of the cycle while intrinsic excitability is increased. In early proestrus (also called proestrus AM), excitatory synapse properties are elevated and intrinsic excitability is decreased. In late proestrus (also called proestrus PM), excitatory synapse properties are drastically reduced and intrinsic excitability properties remain comparable to those in early proestrus and estrus. In the estrus phase, excitatory synapses recover to levels seen in early proestrus while intrinsic excitability is decreased, and levels are comparable to those in early and late proestrus. FSH, follicle-stimulating hormone; LH, luteinizing hormone.

of estrus, and then rises again by diestrus (Naftolin et al. 2007; Olmos et al. 1989). This change in excitatory synapse number is not because of a disappearance of excitatory synapses per se but is rather due to remodeling of astroglia and astroglial processes (García-Segura et al. 1994; Kohama et al. 1995). This idea of fast changes in excitatory synapse properties is not limited to the arcuate nucleus, as a similar but not identical process has also been detected in the anteroventral periventricular nucleus (Langub et al. 1994). If this process is present in the AcbC, then differences in glia and perhaps microglia function should be detectable across the estrous cycle phases. Evidence of microglia sex-specifically altering dopamine inputs in the AcbC during development and puberty has already been presented (Kopec et al. 2018). Further studies could shed light on each of these potential mechanisms. Considered together, a comprehensive action of direct and combinatorial estradiol and progesterone action, a decrease in dendritic spines, and glial ensheathment may collectively act to decrease excitatory synaptic input onto AcbC MSNs during late proestrus, potentially inducing the profound alteration of AcbC MSN excitatory synapse properties.

DISCLOSURES

No conflicts of interest, financial or otherwise, are declared by the authors.

AUTHOR CONTRIBUTIONS

REFERENCES

Adams C, Chen X, Moenter SM. Changes in GABAergic transmission to and intrinsic excitability of gonadotropin-releasing hormone (GnRH) neurons during the estrous cycle in mice. *eNeuro* 5: ENEURO.0171–18.2018, 2018. doi:10.1523/ENEURO.0171-18.2018.

Almey A, Filardo EJ, Milner TA, Brake WG. Estrogen receptors are found in glia and at extranuclear neuronal sites in the dorsal striatum of female rats: evidence for cholinergic but not dopaminergic colocalization. *Endocrinology* 153: 5373–5383, 2012. doi:10.1210/en.2012-1458.

Almey A, Milner TA, Brake WG. Estrogen receptors in the central nervous system and their implication for dopamine-dependent cognition in females. *Horm Behav* 74: 125–138, 2015. doi:10.1016/j.yhbeh.2015.06.010.

Almey A, Milner TA, Brake WG. Estrogen receptor α and G-protein coupled estrogen receptor 1 are localized to GABAergic neurons in the dorsal striatum. *Neurosci Lett* 622: 118–123, 2016. doi:10.1016/j.neulet.2016.04.023.

Alonso-Caraballo Y, Ferrario CR. Effects of the estrous cycle and ovarian hormones on cue-triggered motivation and intrinsic excitability of medium spiny neurons in the nucleus accumbens core of female rats. *Horm Behav* 116: 104583, 2019. doi:10.1016/j.yhbeh.2019.104583.

Bäckström T, Bixo M, Johansson M, Nyberg S, Ossewaarde L, Ragagnin G, Savic I, Strömberg J, Timby E, van Broekhoven F, van Wingen G. Allopregnanolone and mood disorders. *Prog Neurobiol* 113: 88–94, 2014. doi:10.1016/j.pneurobio.2013.07.005.

Bäckström T, Haage D, Löfgren M, Johansson IM, Strömberg J, Nyberg S, Andréen L, Ossewaarde L, van Wingen GA, Turkmen S, Bengtsson SK. Paradoxical effects of GABA-A modulators may explain sex steroid induced negative mood symptoms in some persons. *Neuroscience* 191: 46–54, 2011. doi:10.1016/j.neuroscience.2011.03.061.

Baufreton J, Atherton JF, Surmeier DJ, Bevan MD. Enhancement of excitatory synaptic integration by GABAergic inhibition in the subthalamic nucleus. *J Neurosci* 25: 8505–8517, 2005. doi:10.1523/JNEUROSCI.1163-05.2005.

Beach FA. Sexual attractivity, proceptivity, and receptivity in female mammals. *Horm Behav* 7: 105–138, 1976. doi:10.1016/0018-506X(76)90008-8.

Becker JB. Gender differences in dopaminergic function in striatum and nucleus accumbens. *Pharmacol Biochem Behav* 64: 803–812, 1999. doi:10.1016/S0091-3057(99)00168-9.

Becker JB, Breedlove SM, Crews D, McCarthy MM. *Behavioral Endocrinology*. Cambridge, MA: The MIT Press, 2002.

Becker JB, Hu M. Sex differences in drug abuse. *Front Neuroendocrinol* 29: 36–47, 2008. doi:10.1016/j.yfrne.2007.07.003.

Becker JB, Molenda H, Hummer DL. Gender differences in the behavioral responses to cocaine and amphetamine. Implications for mechanisms mediating gender differences in drug abuse. *Ann N Y Acad Sci* 937: 172–187, 2001. doi:10.1111/j.1749-6632.2001.tb03564.x.

Becker JB, Perry AN, Westenbroek C. Sex differences in the neural mechanisms mediating addiction: a new synthesis and hypothesis. *Biol Sex Differ* 3: 14, 2012. doi:10.1186/2042-6410-3-14.

Becker JB, Rudick CN. Rapid effects of estrogen or progesterone on the amphetamine-induced increase in striatal dopamine are enhanced by estrogen priming: a microdialysis study. *Pharmacol Biochem Behav* 64: 53–57, 1999. doi:10.1016/S0091-3057(99)00091-X.

Belleau ML, Warren RA. Postnatal development of electrophysiological properties of nucleus accumbens neurons. *J Neurophysiol* 84: 2204–2216, 2000. doi:10.1152/jn.2000.84.5.2204.

Bitran D, Shiekh M, McLeod M. Anxiolytic effect of progesterone is mediated by the neurosteroid allopregnanolone at brain GABA$_A$ receptors. *J Neuroendocrinol* 7: 171–177, 1995. doi:10.1111/j.1365-2826.1995.tb00744.x.

Blaustein JD. Neuroendocrine regulation of feminine sexual behavior: lessons from rodent models and thoughts about humans. *Annu Rev Psychol* 59: 93–118, 2008. doi:10.1146/annurev.psych.59.103006.093556.

Blume SR, Freedberg M, Vantrease JE, Chan R, Padival M, Record MJ, DeJoseph MR, Urban JH, Rosenkranz JA. Sex- and estrus-dependent differences in rat basolateral amygdala. *J Neurosci* 37: 10567–10586, 2017. doi:10.1523/JNEUROSCI.0758-17.2017.

Cabrera RJ, Navarro CE. Progesterone in vitro increases NMDA-evoked [^{3}H]dopamine release from striatal slices in proestrus rats. *Neuropharmacology* 35: 175–178, 1996. doi:10.1016/0028-3908(95)00152-2.

Calipari ES, Juarez B, Morel C, Walker DM, Cahill ME, Ribeiro E, Roman-Ortiz C, Ramakrishnan C, Deisseroth K, Han MH, Nestler EJ. Dopaminergic dynamics underlying sex-specific cocaine reward. *Nat Commun* 8: 13877, 2017. doi:10.1038/ncomms13877.

Cao J, Dorris DM, Meitzen J. Neonatal masculinization blocks increased excitatory synaptic input in female rat nucleus accumbens core. *Endocrinology* 157: 3181–3196, 2016. doi:10.1210/en.2016-1160.

Cao J, Willett JA, Dorris DM, Meitzen J. Sex differences in medium spiny neuron excitability and glutamatergic synaptic input: heterogeneity across striatal regions and evidence for estradiol-dependent sexual differentiation. *Front Endocrinol (Lausanne)* 9: 173, 2018. doi:10.3389/fendo.2018.00173.

Chao A, Schlinger BA, Remage-Healey L. Combined liquid and solid-phase extraction improves quantification of brain estrogen content. *Front Neuroanat* 5: 57, 2011. doi:10.3389/fnana.2011.00057.

Deroche MA, Lassalle O, Castell L, Valjent E, Manzoni OJ. Cell-type- and endocannabinoid-specific synapse connectivity in the adult nucleus accumbens core. *J Neurosci* 40: 1028–1041, 2020. doi:10.1523/JNEUROSCI.1100-19.2019.

Dluzen DE, Ramirez VD. Bimodal effect of progesterone on in vitro dopamine function of the rat corpus striatum. *Neuroendocrinology* 39: 149–155, 1984. doi:10.1159/000123971.

Dluzen DE, Ramirez VD. Progesterone effects upon dopamine release from the corpus striatum of female rats. I. Evidence for interneuronal control. *Brain Res* 476: 332–337, 1989a. doi:10.1016/0006-8993(89)91254-7.

Dluzen DE, Ramirez VD. Progesterone effects upon dopamine release from the corpus striatum of female rats. II. Evidence for a membrane site of action and the role of albumin. *Brain Res* 476: 338–344, 1989b. doi:10.1016/0006-8993(89)91255-9.

Dorris DM, Cao J, Willett JA, Hauser CA, Meitzen J. Intrinsic excitability varies by sex in prepubertal striatal medium spiny neurons. *J Neurophysiol* 113: 720–729, 2015. doi:10.1152/jn.00687.2014.

Erskine MS. Solicitation behavior in the estrous female rat: a review. *Horm Behav* 23: 473–502, 1989. doi:10.1016/0018-506X(89)90037-8.

Evans SM, Foltin RW. Exogenous progesterone attenuates the subjective effects of smoked cocaine in women, but not in men. *Neuropsychopharmacology* 31: 659–674, 2006. doi:10.1038/sj.npp.1300887.

Farries MA, Meitzen J, Perkel DJ. Electrophysiological properties of neurons in the basal ganglia of the domestic chick: conservation and divergence in the evolution of the avian basal ganglia. *J Neurophysiol* 94: 454–467, 2005. doi:10.1152/jn.00539.2004.

Farries MA, Perkel DJ. Electrophysiological properties of avian basal ganglia neurons recorded in vitro. *J Neurophysiol* 84: 2502–2513, 2000. doi:10.1152/jn.2000.84.5.2502.

Farries MA, Perkel DJ. A telencephalic nucleus essential for song learning contains neurons with physiological characteristics of both striatum and globus pallidus. *J Neurosci* 22: 3776–3787, 2002. doi:10.1523/JNEUROSCI.22-09-03776.2002.

Floresco SB. The nucleus accumbens: an interface between cognition, emotion, and action. *Annu Rev Psychol* 66: 25–52, 2015. doi:10.1146/annurev-psych-010213-115159.

Forlano PM, Woolley CS. Quantitative analysis of pre- and postsynaptic sex differences in the nucleus accumbens. *J Comp Neurol* 518: 1330–1348, 2010. doi:10.1002/cne.22279.

Francis TC, Lobo MK. Emerging role for nucleus accumbens medium spiny neuron subtypes in depression. *Biol Psychiatry* 81: 645–653, 2017. doi:10.1016/j.biopsych.2016.09.007.

García-Segura LM, Chowen JA, Párducz A, Naftolin F. Gonadal hormones as promoters of structural synaptic plasticity: cellular mechanisms. *Prog Neurobiol* 44: 279–307, 1994. doi:10.1016/0301-0082(94)90042-6.

Grove-Strawser D, Boulware MI, Mermelstein PG. Membrane estrogen receptors activate the metabotropic glutamate receptors mGluR5 and mGluR3 to bidirectionally regulate CREB phosphorylation in female rat striatal neurons. *Neuroscience* 170: 1045–1055, 2010. doi:10.1016/j.neuroscience.2010.08.012.

Hedges VL, Chen G, Yu L, Krentzel AA, Starrett JR, Zhu JN, Suntharalingam P, Remage-Healey L, Wang JJ, Ebner TJ, Mermelstein PG. Local estrogen synthesis regulates parallel fiber-purkinje cell neurotransmission within the cerebellar cortex. *Endocrinology* 159: 1328–1338, 2018. doi:10.1210/en.2018-00039.

Horvath TL, Roa-Pena L, Jakab RL, Simpson ER, Naftolin F. Aromatase in axonal processes of early postnatal hypothalamic and limbic areas including the cingulate cortex. *J Steroid Biochem Mol Biol* 61: 349–357, 1997. doi:10.1016/S0960-0760(97)80032-5.

Hubscher CH, Brooks DL, Johnson JR. A quantitative method for assessing stages of the rat estrous cycle. *Biotech Histochem* 80: 79–87, 2005. doi:10.1080/10520290500138422.

Jakab RL, Horvath TL, Leranth C, Harada N, Naftolin F. Aromatase immunoreactivity in the rat brain: gonadectomy-sensitive hypothalamic neurons and an unresponsive "limbic ring" of the lateral septum-bed nucleus-amygdala complex. *J Steroid Biochem Mol Biol* 44: 481–498, 1993. doi:10.1016/0960-0760(93)90253-S.

Jenkins WJ, Becker JB. Role of the striatum and nucleus accumbens in paced copulatory behavior in the female rat. *Behav Brain Res* 121: 119–128, 2001. doi:10.1016/S0166-4328(00)00394-6.

Ke FC, Ramirez VD. Binding of progesterone to nerve cell membranes of rat brain using progesterone conjugated to 125I-bovine serum albumin as a ligand. *J Neurochem* 54: 467–472, 1990. doi:10.1111/j.1471-4159.1990.tb01895.x.

Kohama SG, Goss JR, McNeill TH, Finch CE. Glial fibrillary acidic protein mRNA increases at proestrus in the arcuate nucleus of mice. *Neurosci Lett* 183: 164–166, 1995. doi:10.1016/0304-3940(94)11141-5.

Kopec AM, Smith CJ, Ayre NR, Sweat SC, Bilbo SD. Microglial dopamine receptor elimination defines sex-specific nucleus accumbens development and social behavior in adolescent rats. *Nat Commun* 9: 3769, 2018. doi:10.1038/s41467-018-06118-z.

Kow LM, Pfaff DW. Effects of estrogen treatment on the size of receptive field and response threshold of pudendal nerve in the female rat. *Neuroendocrinology* 13: 299–313, 1973. doi:10.1159/000122214.

Krentzel AA, Barrett LR, Meitzen J. Estradiol rapidly modulates excitatory synapse properties in a sex- and region-specific manner in rat nucleus accumbens core and caudate-putamen. *J Neurophysiol* 122: 1213–1225, 2019. doi:10.1152/jn.00264.2019.

Krentzel AA, Meitzen J. Biological sex, estradiol and striatal medium spiny neuron physiology: a mini-review. *Front Cell Neurosci* 12: 492, 2018. doi:10.3389/fncel.2018.00492.

Krentzel AA, Proaño S, Patisaul HB, Meitzen J. Temporal and bidirectional influences of estradiol on voluntary wheel running in adult female and male rats. *Horm Behav* 120: 104694, 2020. doi:10.1016/j.yhbeh.2020.104694.

Langub MC Jr, Maley BE, Watson RE Jr. Estrous cycle-associated axosomatic synaptic plasticity upon estrogen receptive neurons in the rat preoptic area. *Brain Res* 641: 303–310, 1994. doi:10.1016/0006-8993(94)90159-7.

Lebron-Milad K, Milad MR. Sex differences, gonadal hormones and the fear extinction network: implications for anxiety disorders. *Biol Mood Anxiety Disord* 2: 3, 2012. doi:10.1186/2045-5380-2-3.

Mani SK, Reyna AM, Alejandro MA, Crowley J, Markaverich BM. Disruption of male sexual behavior in rats by tetrahydrofurandiols (THF-diols). *Steroids* 70: 750–754, 2005. doi:10.1016/j.steroids.2005.04.004.

Markaverich B, Mani S, Alejandro MA, Mitchell A, Markaverich D, Brown T, Velez-Trippe C, Murchison C, O'Malley B, Faith R. A novel endocrine-disrupting agent in corn with mitogenic activity in human breast and prostatic cancer cells. *Environ Health Perspect* 110: 169–177, 2002. doi:10.1289/ehp.02110169.

McEwen BS, Woolley CS. Estradiol and progesterone regulate neuronal structure and synaptic connectivity in adult as well as developing brain. *Exp Gerontol* 29: 431–436, 1994. doi:10.1016/0531-5565(94)90022-1.

Meisel RL, Mullins AJ. Sexual experience in female rodents: cellular mechanisms and functional consequences. *Brain Res* 1126: 56–65, 2006. doi:10.1016/j.brainres.2006.08.050.

Meitzen J, Meisel RL, Mermelstein PG. Sex differences and the effects of estradiol on striatal function. *Curr Opin Behav Sci* 23: 42–48, 2018. doi:10.1016/j.cobeha.2018.03.007.

Meitzen J, Pflepsen KR, Stern CM, Meisel RL, Mermelstein PG. Measurements of neuron soma size and density in rat dorsal striatum, nucleus accumbens core and nucleus accumbens shell: differences between striatal region and brain hemisphere, but not sex. *Neurosci Lett* 487: 177–181, 2011. doi:10.1016/j.neulet.2010.10.017.

Meitzen J, Weaver AL, Brenowitz EA, Perkel DJ. Plastic and stable electrophysiological properties of adult avian forebrain song-control neurons across changing breeding conditions. *J Neurosci* 29: 6558–6567, 2009. doi:10.1523/JNEUROSCI.5571-08.2009.

Mermelstein PG, Becker JB, Surmeier DJ. Estradiol reduces calcium currents in rat neostriatal neurons via a membrane receptor. *J Neurosci* 16: 595–604, 1996. doi:10.1523/JNEUROSCI.16-02-00595.1996.

Micevych PE, Mermelstein PG, Sinchak K. Estradiol membrane-initiated signaling in the brain mediates reproduction. *Trends Neurosci* 40: 654–666, 2017. doi:10.1016/j.tins.2017.09.001.

Milad MR, Igoe SA, Lebron-Milad K, Novales JE. Estrous cycle phase and gonadal hormones influence conditioned fear extinction. *Neuroscience* 164: 887–895, 2009. doi:10.1016/j.neuroscience.2009.09.011.

Miller CK, Krentzel AA, Patisaul HB, Meitzen J. Metabotropic glutamate receptor subtype 5 (mGlu$_5$) is necessary for estradiol mitigation of light-induced anxiety behavior in female rats. *Physiol Behav* 214: 112770, 2020. doi:10.1016/j.physbeh.2019.112770.

Mu P, Moyer JT, Ishikawa M, Zhang Y, Panksepp J, Sorg BA, Schlüter OM, Dong Y. Exposure to cocaine dynamically regulates the intrinsic membrane excitability of nucleus accumbens neurons. *J Neurosci* 30: 3689–3699, 2010. doi:10.1523/JNEUROSCI.4063-09.2010.

Naftolin F, Garcia-Segura LM, Horvath TL, Zsarnovszky A, Demir N, Fadiel A, Leranth C, Vondracek-Klepper S, Lewis C, Chang A, Parducz A. Estrogen-induced hypothalamic synaptic plasticity and pituitary sensitization in the control of the estrogen-induced gonadotrophin surge. *Reprod Sci* 14: 101–116, 2007. doi:10.1177/1933719107301059.

Nowak L, Bregestovski P, Ascher P, Herbet A, Prochiantz A. Magnesium gates glutamate-activated channels in mouse central neurones. *Nature* 307: 462–465, 1984. doi:10.1038/307462a0.

O'Donnell P, Grace AA. Physiological and morphological properties of accumbens core and shell neurons recorded in vitro. *Synapse* 13: 135–160, 1993. doi:10.1002/syn.890130206.

Olmos G, Naftolin F, Perez J, Tranque PA, Garcia-Segura LM. Synaptic remodeling in the rat arcuate nucleus during the estrous cycle. *Neuroscience* 32: 663–667, 1989. doi:10.1016/0306-4522(89)90288-1.

Perry AN, Westenbroek C, Becker JB. Impact of pubertal and adult estradiol treatments on cocaine self-administration. *Horm Behav* 64: 573–578, 2013. doi:10.1016/j.yhbeh.2013.08.007.

Peterson BM, Mermelstein PG, Meisel RL. Estradiol mediates dendritic spine plasticity in the nucleus accumbens core through activation of mGluR5. *Brain Struct Funct* 220: 2415–2422, 2015. doi:10.1007/s00429-014-0794-9.

Piechota M, Korostynski M, Golda S, Ficek J, Jantas D, Barbara Z, Przewlocki R. Transcriptional signatures of steroid hormones in the striatal neurons and astrocytes. *BMC Neurosci* 18: 37, 2017. doi:10.1186/s12868-017-0352-5.

Proaño SB, Morris HJ, Kunz LM, Dorris DM, Meitzen J. Estrous cycle-induced sex differences in medium spiny neuron excitatory synaptic transmission and intrinsic excitability in adult rat nucleus accumbens core. *J Neurophysiol* 120: 1356–1373, 2018. doi:10.1152/jn.00263.2018.

Russo SJ, Festa ED, Fabian SJ, Gazi FM, Kraish M, Jenab S, Quiñones-Jenab V. Gonadal hormones differentially modulate cocaine-induced conditioned place preference in male and female rats. *Neuroscience* 120: 523–533, 2003. doi:10.1016/S0306-4522(03)00317-8.

Salgado S, Kaplitt MG. The nucleus accumbens: a comprehensive review. *Stereotact Funct Neurosurg* 93: 75–93, 2015. doi:10.1159/000368279.

Sofuoglu M, Babb DA, Hatsukami DK. Effects of progesterone treatment on smoked cocaine response in women. *Pharmacol Biochem Behav* 72: 431–435, 2002. doi:10.1016/S0091-3057(02)00716-5.

Sterling RJ, Gasc JM, Sharp PJ, Renoir JM, Tuohimaa P, Baulieu EE. The distribution of nuclear progesterone receptor in the hypothalamus and forebrain of the domestic hen. *Cell Tissue Res* 248: 201–205, 1987. doi:10.1007/BF01239981.

Terasawa E, Timiras PS. Electrical activity during the estrous cycle of the rat: cyclic changes in limbic structures. *Endocrinology* 83: 207–216, 1968. doi:10.1210/endo-83-2-207.

Tien NW, Kerschensteiner D. Homeostatic plasticity in neural development. *Neural Dev* 13: 9, 2018. doi:10.1186/s13064-018-0105-x.

Tonn Eisinger KR, Larson EB, Boulware MI, Thomas MJ, Mermelstein PG. Membrane estrogen receptor signaling impacts the reward circuitry of the female brain to influence motivated behaviors. *Steroids* 133: 53–59, 2018. doi:10.1016/j.steroids.2017.11.013.

Tozzi A, de Iure A, Tantucci M, Durante V, Quiroga-Varela A, Giampà C, Di Mauro M, Mazzocchetti P, Costa C, Di Filippo M, Grassi S, Pettorossi VE, Calabresi P. Endogenous 17β-estradiol is required for activity-dependent long-term potentiation in the striatum: interaction with the dopaminergic system. *Front Cell Neurosci* 9: 192, 2015. doi:10.3389/fncel.2015.00192.

Turrigiano G. Homeostatic synaptic plasticity: local and global mechanisms for stabilizing neuronal function. *Cold Spring Harb Perspect Biol* 4: a005736, 2012. doi:10.1101/cshperspect.a005736.

Tuscher JJ, Szinte JS, Starrett JR, Krentzel AA, Fortress AM, Remage-Healey L, Frick KM. Inhibition of local estrogen synthesis in the hippocampus impairs hippocampal memory consolidation in ovariectomized female mice. *Horm Behav* 83: 60–67, 2016. doi:10.1016/j.yhbeh.2016.05.001.

Villalon Landeros R, Morisseau C, Yoo HJ, Fu SH, Hammock BD, Trainor BC. Corncob bedding alters the effects of estrogens on aggressive behavior and reduces estrogen receptor-α expression in the brain. *Endocrinology* 153: 949–953, 2012. doi:10.1210/en.2011-1745.

Wagner CK, Morrell JI. Distribution and steroid hormone regulation of aromatase mRNA expression in the forebrain of adult male and female rats: a cellular-level analysis using in situ hybridization. *J Comp Neurol* 370: 71–84, 1996. doi:10.1002/(SICI)1096-9861(19960617)370:1<71:AID-CNE7>3.0.CO;2-I.

Westwood FR. The female rat reproductive cycle: a practical histological guide to staging. *Toxicol Pathol* 36: 375–384, 2008. doi:10.1177/0192623308315665.

Willett JA, Cao J, Johnson A, Patel OH, Dorris DM, Meitzen J. The estrous cycle modulates rat caudate-putamen medium spiny neuron physiology. *Eur J Neurosci*. 2019. doi:10.1111/ejn.14506.

Willett JA, Will T, Hauser CA, Dorris DM, Cao J, Meitzen J. No evidence for sex differences in the electrophysiological properties and excitatory synaptic input onto nucleus accumbens shell medium spiny neurons. *eNeuro* 3: ENEURO.0147–15.2016, 2016. doi:10.1523/ENEURO.0147-15.2016.

Wissman AM, May RM, Woolley CS. Ultrastructural analysis of sex differences in nucleus accumbens synaptic connectivity. *Brain Struct Funct* 217: 181–190, 2012. doi:10.1007/s00429-011-0353-6.

Wong JE, Cao J, Dorris DM, Meitzen J. Genetic sex and the volumes of the caudate-putamen, nucleus accumbens core and shell: original data and a review. *Brain Struct Funct* 221: 4257–4267, 2016. doi:10.1007/s00429-015-1158-9.

Woolley CS, McEwen BS. Roles of estradiol and progesterone in regulation of hippocampal dendritic spine density during the estrous cycle in the rat. *J Comp Neurol* 336: 293–306, 1993. doi:10.1002/cne.903360210.

Yoest KE, Cummings JA, Becker JB. Estradiol, dopamine and motivation. *Cent Nerv Syst Agents Med Chem* 14: 83–89, 2014. doi:10.2174/1871524914666141226103135.

Yoest KE, Quigley JA, Becker JB. Rapid effects of ovarian hormones in dorsal striatum and nucleus accumbens. *Horm Behav* 104: 119–129, 2018. doi:10.1016/j.yhbeh.2018.04.002.